JCB Journal of Cell Biology

ARTICLE

Deubiquitinases USP20/33 promote the biogenesis of tail-anchored membrane proteins

Jacob A. Culver and Malaiyalam Mariappan

Numerous proteins that have hydrophobic transmembrane domains (TMDs) traverse the cytosol and posttranslationally insert into cellular membranes. It is unclear how these hydrophobic membrane proteins evade recognition by the cytosolic protein quality control (PQC), which typically recognizes exposed hydrophobicity in misfolded proteins and marks them for proteasomal degradation by adding ubiquitin chains. Here, we find that tail-anchored (TA) proteins, a vital class of membrane proteins, are recognized by cytosolic PQC and are ubiquitinated as soon as they are synthesized in cells. Surprisingly, the ubiquitinated TA proteins are not routed for proteasomal degradation but instead are handed over to the targeting factor, TRC40, and delivered to the ER for insertion. The ER-associated deubiquitinases, USP20 and USP33, remove ubiquitin chains from TA proteins after their insertion into the ER. Thus, our data suggest that deubiquitinases rescue posttranslationally targeted membrane proteins that are inappropriately ubiquitinated by PQC in the cytosol.

Introduction

Membrane proteins are essential for eukaryotic life, but there are challenges particular to the synthesis and insertion of membrane proteins (Shao and Hegde, 2011). Membrane proteins contain hydrophobic transmembrane domains (TMDs) that typically reside within a membrane and are thus shielded from the aqueous cytosol; however, nearly all membrane proteins begin their synthesis in the cytosol. This raises the problem of exposing and aggregating hydrophobic TMDs in the aqueous cytosol during their synthesis, damaging cellular protein homeostasis (Hegde and Zavodszky, 2019). Evolution solved this problem by coupling protein synthesis and insertion at the ER, where the majority of membrane proteins are synthesized (Cymer et al., 2015). These proteins typically contain either an N-terminal signal sequence or TMD that is cotranslationally recognized by the signal recognition particle (SRP) in the cytosol (Zhang and Shan, 2014). The SRP-bound ribosome-nascent chain complex is then delivered to the ER-localized SRP receptor, and the nascent chain is cotranslationally integrated into the membrane via the Sec61 translocon pore (Rapoport, 2007).

There are exceptions to the cotranslational protein insertion pathway. Tail-anchored (TA) membrane proteins are an essential class of proteins that are precluded from SRP binding upon translation (Kutay et al., 1995; Kutay et al., 1993). TA proteins are distinguishable by their singular TMDs located at their carboxy-terminus. When the C-terminal TMD of a nascent TA protein emerges from the ribosome exit tunnel, SRP is unable to bind and pause translation because translation has already terminated (Kutay et al., 1995); therefore, the nascent TA protein is released into the cytosol, and additional factors are needed to shield the hydrophobic TA membrane domain and deliver it to the correct membrane. TA proteins must be distinguished from misfolded and mislocalized proteins, since protein quality control (PQC) pathways use exposed hydrophobicity as a signal for degradation (Ciechanover and Kwon, 2017; Fredrickson et al., 2013; Xu et al., 2016). Additionally, TA proteins must be sorted to the correct insertion pathway for various membranes, including the ER, mitochondria, and peroxisome (Borgese et al., 2019). TA proteins play critical roles in virtually all aspects of cell biology, such as protein translocation, intracellular trafficking, and programmed cell death (Chacinska et al., 2009; Shamas-Din et al., 2013; Südhof and Rothman, 2009). Thus, a mechanistic understanding of the targeting and maturation of TA proteins is of basic cell biological and physiological significance.

Recent studies have discovered multiple pathways that mediate the targeting of TA proteins to subcellular locations, in particular to the ER (Aviram et al., 2016; Colombo et al., 2009; Favaloro et al., 2008; Guna et al., 2018; Rabu et al., 2008; Stefanovic and Hegde, 2007). The GET (guided entry of tail-anchored proteins) pathway in yeast and the TRC (transmembrane domain recognition complex) pathway in mammals route TA proteins, especially the more hydrophobic ones, to the ER for

Department of Cell Biology, Nanobiology Institute, Yale School of Medicine, West Haven, CT.

Correspondence to Malaiyalam Mariappan: malaiyalam.mariappan@yale.edu.

insertion (Chartron et al., 2012; Chio et al., 2017; Denic et al., 2013; Hegde and Keenan, 2011). In mammals, SGTA (small glutamine-rich tetratricopeptide repeat-containing protein α) first captures the newly synthesized TA proteins and then hands them over to TRC40 (Shao et al., 2017; Wang et al., 2010). The transfer reaction from SGTA to TRC40 is mediated by the BAG6 complex, which is composed of BAG6, TRC35, and Ubl4A (Leznicki et al., 2010; Mariappan et al., 2010; Mock et al., 2015; Shao et al., 2017). The TRC40-bound TA proteins are then delivered to the ER-localized WRB/CAML receptor (tryptophan-rich basic protein and calcium-modulating cyclophilin ligand) complex for insertion (Vilardi et al., 2011; Yamamoto and Sakisaka, 2012). In vitro reconstitution studies have shown that the BAG6 complex can also function as a triaging factor. If SGTA-bound TA proteins are not promptly transferred to TRC40, the BAG6 complex captures such TA proteins and mediates their ubiquitination and subsequent degradation (Hessa et al., 2011; Rodrigo-Brenni et al., 2014; Shao et al., 2017). This triage step has been proposed to distinguish between TA proteins for insertion and mislocalized proteins for degradation; however, it is still unclear how newly synthesized hydrophobic TA proteins escape from recognition and ubiquitination by the cytosolic PQC system, which encompasses a network of chaperones and E3 ubiquitin ligases (Ciechanover and Kwon, 2017). Here, we found that nascent TA proteins are not efficiently shielded from recognition by PQC in the cytosol. Instead, the newly synthesized TA proteins are ubiquitinated in cells and in vitro. Upon further investigation, we found that, despite clear ubiquitination of nascent TA proteins, few were actually degraded. In fact, ubiquitinated TA proteins were still transferred to TRC40 and inserted, and the insertion was closely timed with deubiquitination. The contrast between ubiquitinated TA proteins in the cytosol and minimal ubiquitinated TA proteins at the ER membrane led to our discovery that ER-associated deubiquitinases (DUBs) USP20 and USP33 deubiquitinate TA proteins at the ER membrane. Taken together, our data suggest that nascent TA proteins are ubiquitinated in the cytosol, whereupon they are captured and deubiquitinated both before and after insertion into the ER membrane.

Results

Newly synthesized TA proteins are ubiquitinated in cells

A hallmark of the cotranslational protein insertion pathway is that protein synthesis and insertion of TMDs are coupled at the ER membrane (Cymer et al., 2015). This precludes the exposure of TMDs to the cytosol; however, numerous nascent TA proteins that have hydrophobic C-TMDs are released into the cytosol and are posttranslationally inserted into cellular membranes. The cytosol harbors an extensive PQC network, which often recognizes exposed hydrophobicity of misfolded or mislocalized proteins and marks them for proteasomal degradation by adding ubiquitin chains; therefore, we asked how cells can distinguish between degradation and insertion substrates. We hypothesized that, if TA proteins are shielded from cytosolic PQC machinery, they should not be ubiquitinated and degraded in cells. To test this, we constructed TA proteins that vary in the hydrophobicity of their C-terminal TMDs (Fig. S1 A). First, we examined whether newly synthesized TA proteins are ubiquitinated in the cytosol before their targeting and insertion into the ER membrane. In vitro translation of the TA protein, Sec61β, a component of the Sec61 translocon, in rabbit reticulocyte lysate (RRL) resulted in modifications consistent with ubiquitination of Sec61β (Fig. 1 A), which matches with the previous study (Hessa et al., 2011). The ubiquitination was dependent on the TMD, since its removal resulted in a significant loss of ubiquitination. Although dependent on the TMD, the ubiquitination should occur on the cytosolic domain of Sec61β, since the TMD lacks lysine residues for ubiquitination (Fig. S1 A).

Since TA protein ubiquitination has only been observed in vitro (Hessa et al., 2011; Shao et al., 2017), we asked whether this occurs in cultured cells. To address this, we cotransfected HEK293 cells with HA-ubiquitin and FLAG-tagged VAPA (VAMP-associated protein A), an abundant TA protein that plays a central role in mediating ER-membrane contact sites (Murphy and Levine, 2016). The cell lysates were immunoprecipitated for VAPA using radioimmunoprecipitation assay (RIPA) buffer to remove most protein–protein interactions and probed for ubiquitinated VAPA with anti-HA antibodies. Consistent with in vitro data, the immunoblotting analysis showed that VAPA was ubiquitin modified in a C-terminal TMD-dependent manner in cells (Fig. 1 B). The insertion of VAPA into the ER membrane was mirrored by N-glycosylation—indicated by an orange dot—of the engineered N-glycan acceptor motif introduced at the C-terminus of VAPA. The N-glycosylation of VAPA was verified by its sensitivity to endoglycosidase H (Endo H; Fig. S1 B). We also detected TA protein ubiquitination when cells were harvested in hot SDS buffer and immunoprecipitated after dilution, which argues that TA protein ubiquitination is not a postlysis artifact (Fig. S1 C). Also, ubiquitination was not due to transient overexpression of TA proteins, because the ubiquitination could be detected from cells stably expressing a TA protein (Fig. S1 D). The cytosolic PQC selectively recognizes the TMD of a TA protein for ubiquitination since appending the VAMP2 (vesicle-associated membrane protein 2) TMD to the soluble protein DHFR (dihydrofolate reductase) led to ubiquitination (Fig. 1 C). Although all TA proteins have a single TMD at their C-terminus, their hydrophobicity varies greatly among substrates (Fig. S1 A). We reasoned that more hydrophobic TA proteins may be more attractive substrates for the cytosolic PQC machinery in cells and therefore show stronger ubiquitin signals. To test this, we constructed fusion constructs where we swapped the TMD of Sec61β with either VAMP2 TMD or VAMP2 hydrophobic TMD, in which less hydrophobic amino acids were replaced with more hydrophobic amino acids (Fig. S1 A). Since they all contain the same cytosolic domain of Sec61β, these constructs allowed us to specifically determine the role of TMD hydrophobicity in mediating ubiquitination. Indeed, we found that the hydrophobic VAMP2 construct showed strong ubiquitination, even though the level of total protein was less than other constructs. In contrast, the less hydrophobic construct Sec61β showed a moderate level of ubiquitination (Figs. 1 D and S1 A).

We next asked whether TA proteins are ubiquitinated in the cytosol or at the ER membrane. To address this, we fractionated

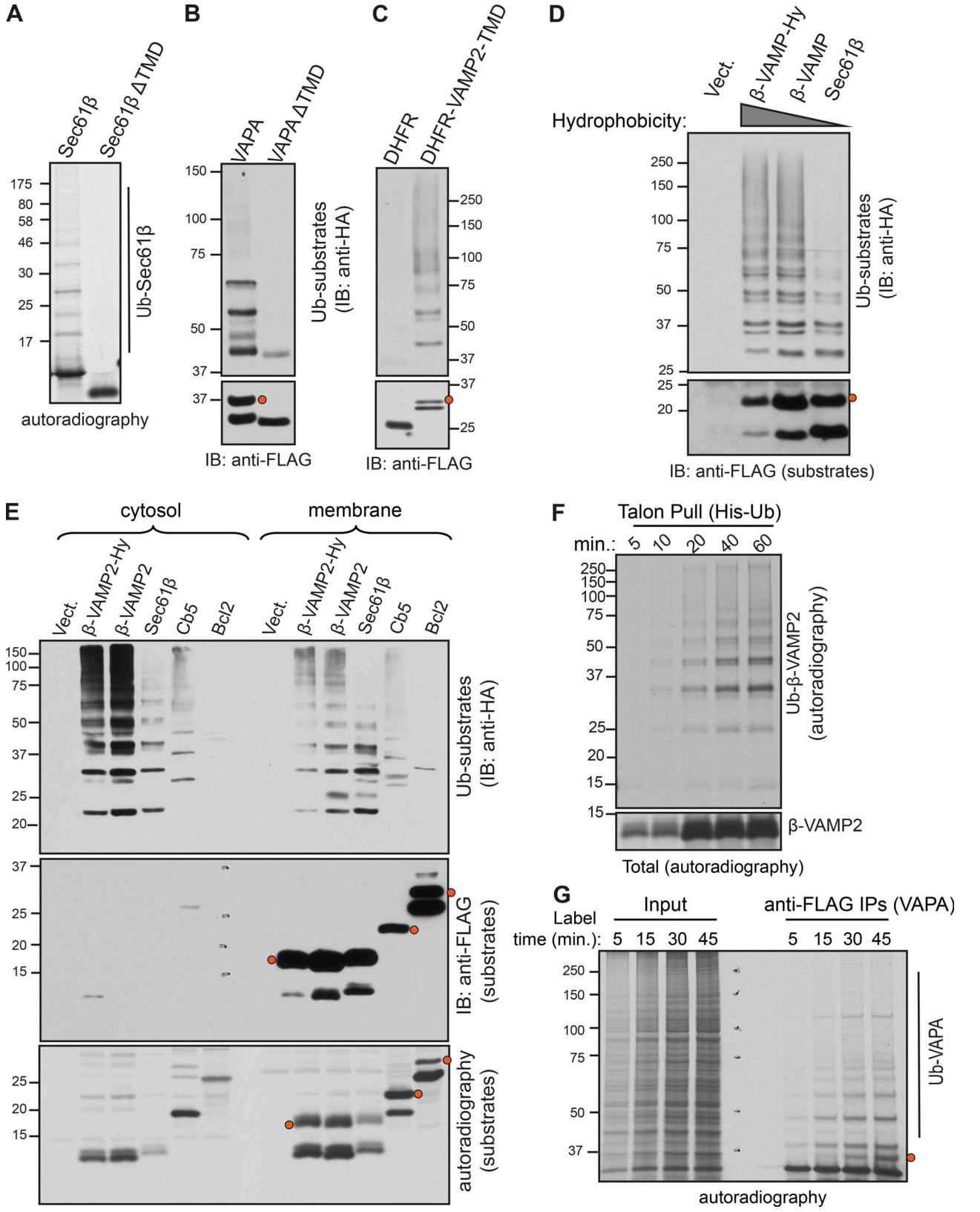

Figure 1. **Nascent TA proteins are ubiquitinated in the cytosol. (A)** Sec61β-encoding transcripts were translated in RRL and directly analyzed by SDS-PAGE autoradiography. **(B)** FLAG-tagged VAPA or VAPA lacking its TMD was transfected along with HA-ubiquitin (Ub) into HEK293 cells. The lysates were immunoprecipitated (IP) with anti-FLAG beads and analyzed by immunoblotting (IB) with anti-HA for ubiquitinated substrates and anti-FLAG for VAPA. The orange circle indicates the inserted form of VAPA that was glycosylated due to its C-terminal glycosylation motif. **(C)** FLAG-tagged DHFR or DHFR fused with the VAMP2 TMD was transfected and analyzed as in B. Data are representative of two independent experiments. **(D)** The indicated constructs with varying

hydrophobicity of TMDs were transfected and analyzed as in B. **(E)** The cells transfected with the indicated constructs and HA-ubiquitin were metabolically labeled and fractionated into cytosol and membrane using digitonin. Both cytosol and membrane fractions were immunoprecipitated and analyzed by immunoblotting as in B. The immunoprecipitants were also analyzed by autoradiography. **(F)** β-VAMP2–encoding transcripts were in vitro translated in RRL for the noted times and analyzed by SDS-PAGE autoradiography directly (total) or after isolation of His-tagged ubiquitin-conjugated TA proteins using Talon resin. **(G)** Cells expressing FLAG-VAPA were metabolically labeled for the indicated time points and analyzed by autoradiography directly (input) or after immunoprecipitation with anti-FLAG antibodies. Data are representative of two independent experiments.

cells expressing TA proteins using a low concentration of digitonin, which selectively permeabilized the plasma membrane, but not the ER. Even though the total amount of TA proteins in the cytosol was minimal compared with the membrane, immunoblotting of ubiquitinated TA proteins after immunoprecipitation revealed a strong ubiquitination signal in the cytosol fraction compared with the membrane fraction (Fig. 1 E). Newly translated TA proteins reside transiently in the cytosol and are rapidly inserted into the ER membrane; therefore, immunoblotting only detected the larger pool of TA proteins localized in the membrane fraction, but nascent TA proteins were readily detected in the cytosol by radiolabeling, a very sensitive technique that can detect specifically nascent TA proteins (Fig. 1 E). These results suggest that, despite the transient nature and low total yield of cytosolic TA proteins, the majority of the ubiquitin signal comes from this population. Importantly, glycosylated TA proteins were only detected in the membrane fraction, suggesting that the fractionation successfully isolated the cytosolic fraction (Fig. 1 E). Moreover, most ubiquitinated TA proteins were not sensitive to Endo H, suggesting that TA protein ubiquitination occurs in the cytosol before insertion (Fig. S1 B). To determine if the ubiquitination of TA proteins occurs immediately after their synthesis in the cytosol, we in vitro translated the TA proteins in RRL and monitored ubiquitination at various time points. The ubiquitination of β-VAMP2 could be detected within 10 min of translation, and more ubiquitinated β-VAMP2 appeared as the translation time further proceeded (Fig. 1 F). This result also shows that TA ubiquitination occurs independent of any membrane-bound ubiquitination machinery and further supports the idea that nascent TA proteins are ubiquitinated in the cytosol before insertion into the ER. As in the in vitro data, ubiquitinated TA proteins could be directly detected even upon 5 min of labeling in cells, and TA protein ubiquitination continuously increased along with translated TA proteins (Fig. 1 G). Quantification of ubiquitinated VAPA revealed that ∼8% of nascent cytosolic TA proteins are ubiquitinated (Fig. S1 H). Collectively, these results suggest that a small fraction of newly synthesized TA proteins are ubiquitinated in the cytosol before insertion into the ER membrane.

TA proteins carry a K48-linked polyubiquitin chain

The distribution of ubiquitin attached to proteins may vary, as in polyubiquitination or multimonoubiquitination (Komander and Rape, 2012). The type of ubiquitination modification on a protein can determine its downstream fate; we therefore asked whether TA proteins are polyubiquitinated or multimonoubiquitinated in cells. To this end, we generated various lysine mutants of our model substrate β-VAMP2 and monitored their ubiquitination in cells. Polyubiquitination of β-VAMP2 harboring a single lysine residue was similar to β-VAMP2 containing multiple lysine residues, which supports the conclusion that TA proteins are polyubiquitinated in cells (Fig. 2 A). Polyubiquitination can occur on different lysine residues of ubiquitin, and lysine 48 (K48) modification mediates recognition of proteins by the proteasome. To determine the type of polyubiquitination on TA proteins, we performed immunoblotting of immunoprecipitated VAPA from cells using K48-ubiquitin linkage–specific antibodies. Indeed, both anti-ubiquitin and K48 linkage–specific antibodies detected polyubiquitinated VAPA on immunoblots (Fig. 2 B). Although additional forms of ubiquitin linkages may be present, these results suggest that TA proteins are decorated with K48-linked ubiquitin chains that are suitable for recognition by proteasomes.

TA protein ubiquitination is not due to the limitation of cytosolic targeting factors

We next reasoned that if TA protein ubiquitination is caused by the saturation of targeting factors, adding purified recombinant targeting factors should suppress TA protein ubiquitination. To test this, we in vitro translated TA proteins in RRL with increasing concentrations of purified recombinant TRC40, the final targeting factor in the cytosol that delivers TA proteins to the ER membrane for insertion (Fig. 3 A). Adding an excess of TRC40 did not inhibit the ubiquitination of either nascent Sec61β (Fig. 3 B) or β-VAMP2 (Fig. S1 E), which demonstrates that TA protein ubiquitination is not due to a limitation of the targeting factor. We further investigated this idea in cells by overexpressing targeting factors one at a time. Transient overexpression of SGTA or BAG6 did not appreciably influence the ubiquitination of the TA protein (Fig. 3 C); however, overexpressing TRC40 did lead to an increase in TA ubiquitination. This is likely due to slowed insertion, as overexpressed TRC40 may exhibit a dominant-negative effect by binding to ER insertion factors (WRB/CAML) and blocking the TRC40 loaded with TA proteins (Fig. 3 C). Since overexpressing chaperones failed to protect nascent TA proteins from ubiquitination, we asked if one of these chaperones was actually responsible for the ubiquitin signal we observed. Since BAG6 is known to bind to E3 ligase RNF126 (Rodrigo-Brenni et al., 2014), we hypothesized that TA proteins are ubiquitinated via binding to a chaperone known to recruit ubiquitination machinery. Therefore, we knocked out SGTA and BAG6 and created a partial knockout of CAML in HEK293 cells by CRISPR/Cas9. We were unable to knock out TRC40 or completely knock out CAML, presumably because these mutations would be lethal to cells. TA proteins were still able to be inserted as shown by glycosylation in cells lacking SGTA or BAG6 (Fig. S1 F), implying that TRC40 and the WRB/CAML complex are sufficient for the insertion of TA

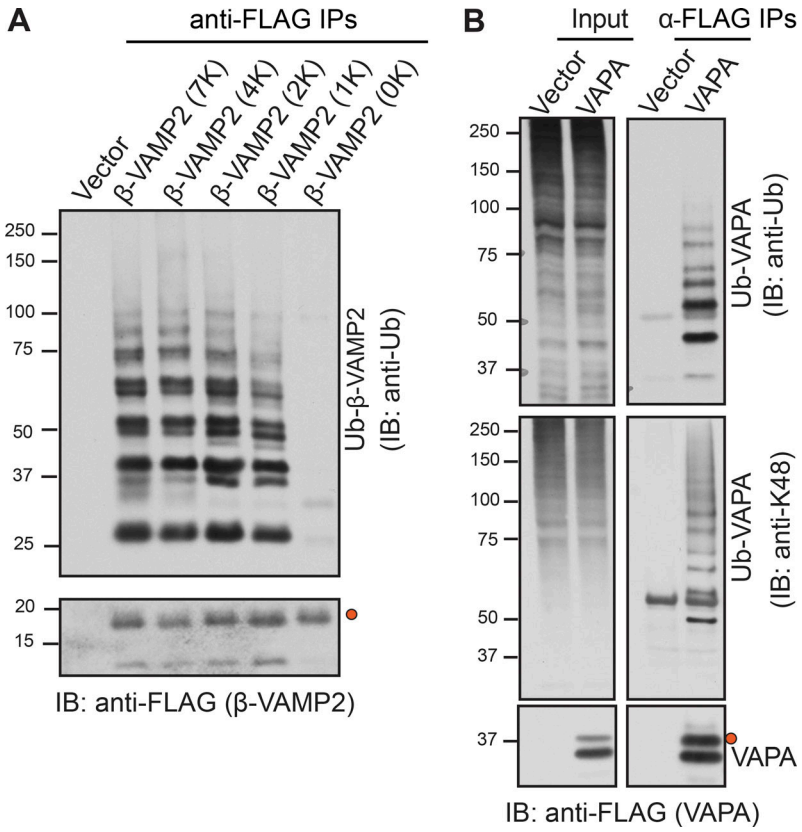

Figure 2. **Characterization of TA protein ubiquitination.** **(A)** β-VAMP2 with progressively more lysine residues mutated to arginine residues were immunoprecipitated (IP) and analyzed by immunoblotting (IB) for β-VAMP2 or ubiquitinated (Ub) β-VAMP2. Data are representative of two independent experiments. **(B)** VAPA was immunoprecipitated and ubiquitinated VAPA was directly analyzed by immunoblotting with either anti-ubiquitin or K48-linkage–specific polyubiquitin antibody.

proteins in cultured cells. Knockout of SGTA had little effect on TA protein ubiquitination (Fig. 3 D). To our surprise, knockout of BAG6 did not show any appreciable defects in TA protein ubiquitination (Fig. 3 D and Fig. S1 G), suggesting that ER-targeted TA proteins can be ubiquitinated independently of BAG6 in cells. By contrast, the partial knockout of CAML drastically increased TA ubiquitination compared with control cells, likely due to the accumulation of nontargeted TA proteins in the cytosol (Fig. 3 D).

Previously, it was proposed that the BAG6 complex, a component of the TA insertion pathway, functioned to triage mislocalized proteins for ubiquitination and degradation while passing TA proteins onto TRC40 for ER insertion (Shao and Hegde, 2016; Shao et al., 2017); however, we observed clear TA ubiquitination regardless of the availability of chaperones. Since ubiquitination is so closely tied to misfolded proteins and degradation, we wanted to rule out the possibility that TA proteins are ubiquitinated because they are not properly handed over to the final targeting factor, TRC40. Immunoprecipitation of endogenous TRC40 revealed that ubiquitinated VAPA could be captured by TRC40 (Fig. 3 E). The endogenous TRC40 selectively bound to the ubiquitinated TA protein, but not to VAPA lacking its TMD. It is unlikely that this result is due to a TRC40–BAG6 interaction, because TRC40 could capture ubiquitinated TA proteins even in the absence of BAG6 in cells (Fig. 3 F). If TRC40 can capture ubiquitinated TA proteins, we should be able to detect the endogenous ubiquitinated proteins associating with the endogenous TRC40. To evaluate this, we passed the cytosol extract of HEK293 cells through anti-TRC40 antibody–conjugated agarose beads and selectively eluted TRC40-associated proteins using Triton X-100 to disrupt hydrophobic interactions between TRC40 and TA proteins. Immunoblotting of eluted samples revealed that the endogenous TRC40 could indeed capture ubiquitinated proteins, which were confirmed by treatment with a promiscuous DUBs, USP2 (Fig. 3 G). Ubiquitinated proteins were slightly increased in CAML-depleted cells compared with WT cells because ubiquitinated TA proteins likely accumulate in the cytosol in the absence of CAML, which is essential for mediating TA protein insertion into the ER. Interestingly, the endogenous VAPA could be detected in TRC40-associated proteins, which confirms that TRC40 substrates are TA proteins (Fig. 3 G). Collectively, these data suggest that ubiquitinated TA proteins are captured by TRC40 for targeting to the ER membrane.

Deubiquitination and insertion of TA proteins are coupled at the ER membrane

The aforementioned data suggest that nascent TA proteins are ubiquitinated in the cytosol regardless of relevant chaperone availability. We reasoned that if ubiquitinated TA proteins are destined for degradation, our model TA substrates should exhibit reduced half-lives. In contrast, pulse-chase experiments revealed that our model TA proteins, β-VAMP2 and VAPA, were very stable up to 8 h of chase (Fig. 4 A). To determine the fate of ubiquitinated TA proteins, we compared VAPA with XBP1(L246A) mutant (XBP1m) using a cycloheximide (CHX) chase combined with a ubiquitination assay. XBP1 is normally targeted to the ER membrane by the SRP pathway (Kanda et al.,

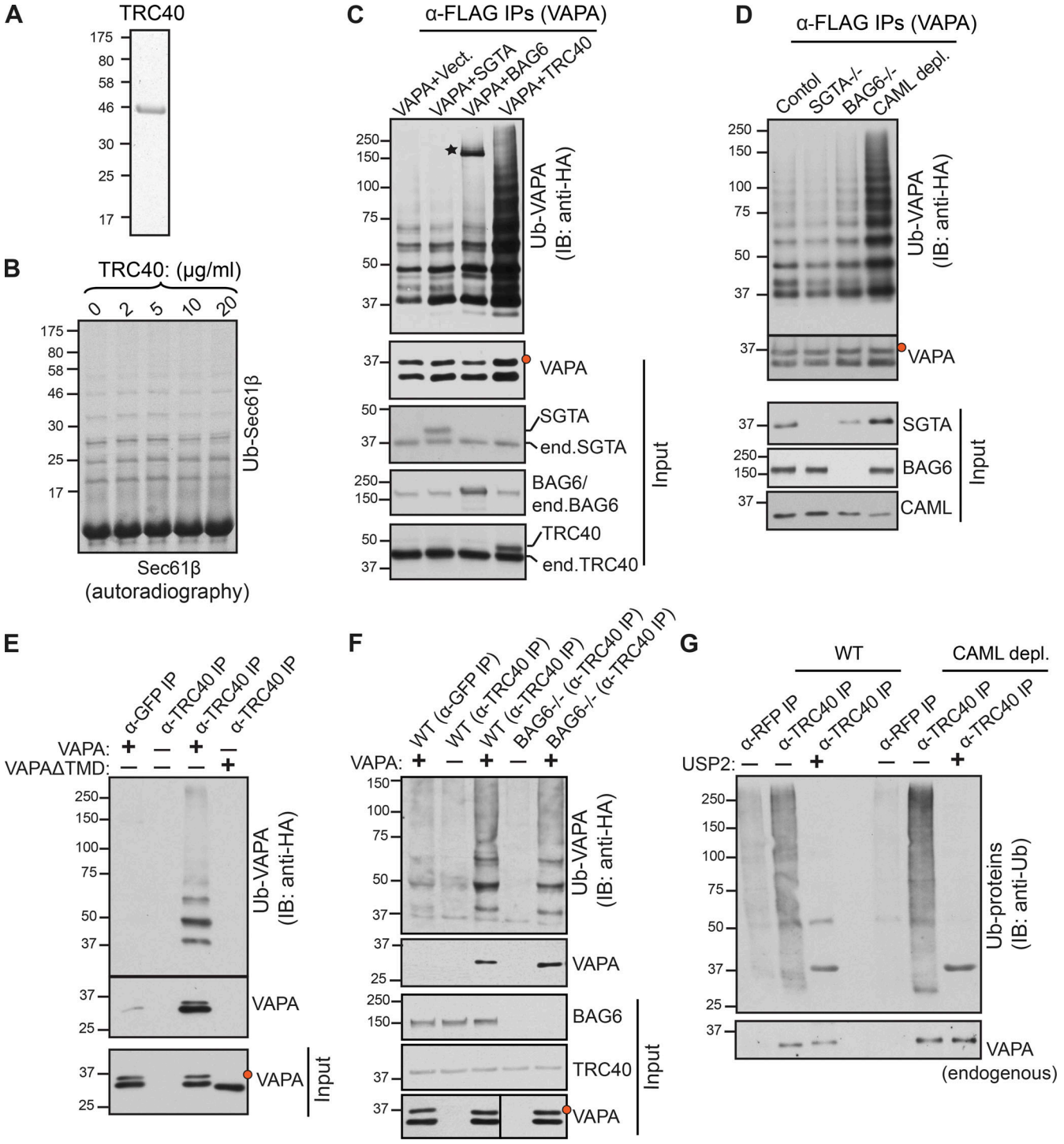

Figure 3. **Chaperone availability does not influence the ubiquitination of TA proteins. (A)** Coomassie blue–stained gel showing the purified recombinant TRC40 from *E. coli*. **(B)** Sec61β-encoding transcripts were in vitro translated in RRL, including increasing concentrations of purified TRC40. The translated products were directly analyzed by autoradiography. **(C)** HEK293 cells were transfected with the indicated constructs along with HA-ubiquitin (Ub). The lysates were either directly analyzed (input) or analyzed after immunoprecipitation (IP) with anti-FLAG beads by immunoblotting (IB) for the indicated antigens. The endogenous proteins were denoted as end. The orange circle indicates the inserted and glycosylated form of VAPA. The star indicates BAG6-FLAG, which was immunoprecipitated with VAPA due to the shared tags. **(D)** The indicated cell lines were transfected with FLAG-VAPA along with HA-ubiquitin and analyzed as in C. **(E)** HEK293 cells were transfected with empty vector, FLAG-VAPA, or FLAG-VAPA ΔTMD along with HA-ubiquitin. The cells were lysed with 0.05% digitonin so as to not disrupt the TRC40–substrate TMD hydrophobic interaction and immunoprecipitated with anti-GFP (control) or anti-TRC40 antibodies. Data are representative of two independent experiments. **(F)** TRC40 was immunoprecipitated and examined as in E with the addition of comparing WT with BAG6$^{-/-}$ HEK293 cells. **(G)** Endogenous cytosolic proteins from HEK293 or CAML-depleted HEK293 cells were isolated using 0.015% digitonin, and TRC40 was purified using anti-TRC40 antibodies conjugated to agarose. Anti-RFP antibodies conjugated to agarose served as a control. TRC40-bound substrates were eluted via 1% Triton X-100 and treated without or with USP2 before analyzing by immunoblotting for the indicated antigens.

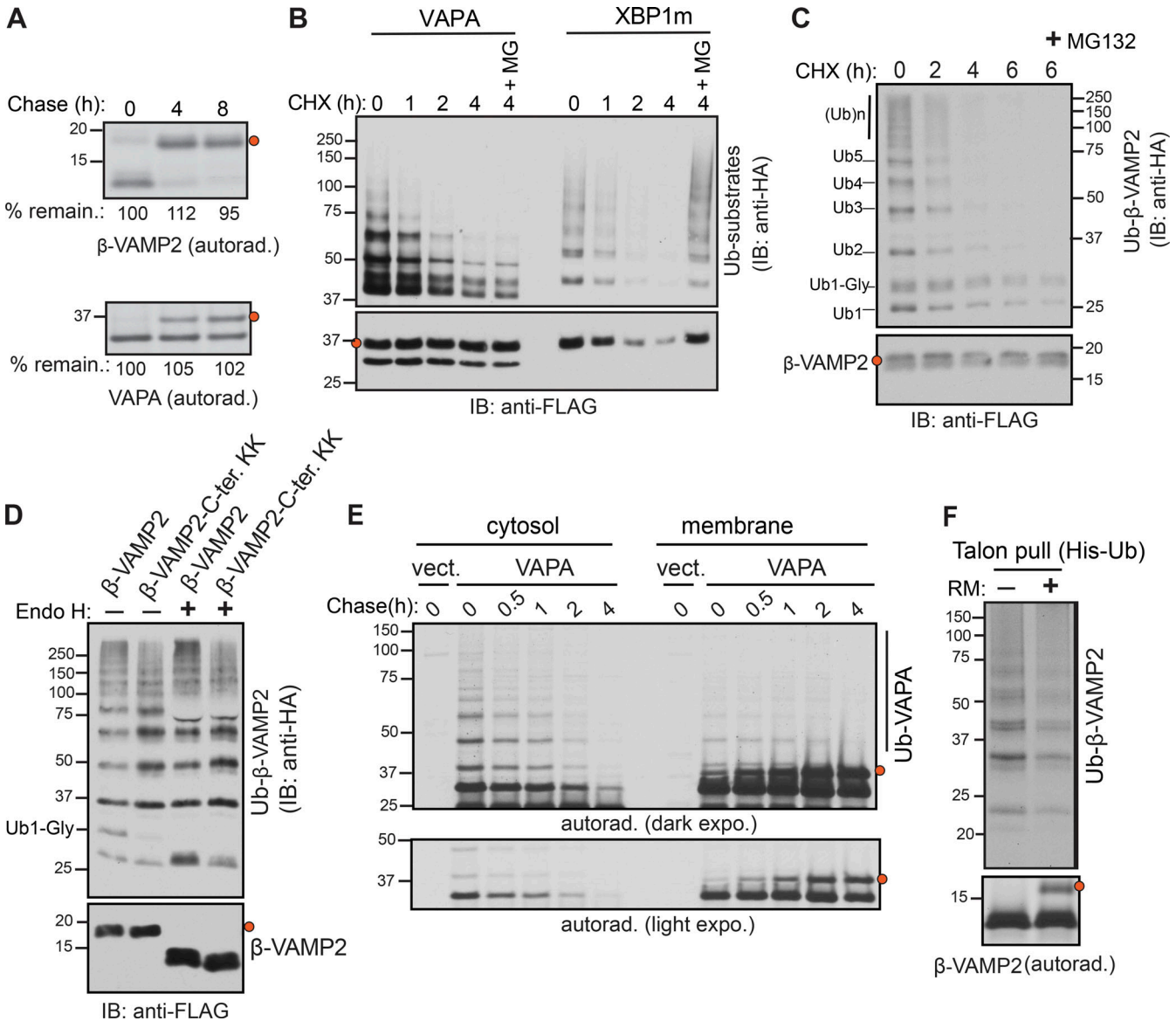

Figure 4. **Ubiquitinated TA proteins are deubiquitinated and inserted into the ER membrane. (A)** FLAG-tagged β-VAMP2– or VAPA-expressing cells were metabolically labeled and chased for the indicated time points. The cell lysates were immunoprecipitated with anti-FLAG beads and analyzed by SDS-PAGE autoradiography. The protein level at 0 h time point was taken as 100%, and the percentage of the remaining protein was calculated with respect to 0 h. The orange circle indicates the glycosylated forms of TA proteins. **(B)** VAPA or a degradation model substrate, XBP1u mutant (L246A), was expressed in HEK293 cells. Cells were treated with CHX alone or with proteasome inhibitor MG132 for the indicated durations. VAPA and XBP1m were immunoprecipitated via anti-FLAG antibody beads and analyzed by immunoblotting (IB) with anti-FLAG for substrates and anti-HA antibody for ubiquitinated (Ub) substrates. Data are representative of two independent experiments. **(C)** FLAG-tagged β-VAMP2– and HA-ubiquitin–expressing cells were treated and analyzed as in B. Note that the monoubiquitinated and glycosylated form of VAMP2 (Ub1-Gly) could be detected, suggesting that DUBs do not efficiently remove all ubiquitin chains before TA protein insertion. **(D)** FLAG–β-VAMP2 or β-VAMP2 C-terminal KK mutant (all lysine residues in the cytosolic domain were replaced with arginine residues, leaving two lysine residues in the C-terminal tail) was transfected along with HA-ubiquitin and immunoprecipitated with anti-FLAG beads and analyzed as in B after treating the samples with or without Endo H. **(E)** FLAG-VAPA–expressing cells were metabolically labeled and chased for the indicated time points. At each time point, cells were permeabilized with digitonin to collect cytosol and membrane fractions. The samples were immunoprecipitated with anti-FLAG beads and analyzed by autoradiography. **(F)** β-VAMP2 was translated in RRL and centrifuged to remove ribosomes. The supernatant was incubated with either buffer or crude rough microsomes derived from HEK293 cells. The samples were analyzed by autoradiography after immunoprecipitating with anti-FLAG beads or isolation of His-tagged ubiquitin-conjugated β-VAMP2 using Talon resin.

2016; Plumb et al., 2015), but a mutation (L246A) in the translational pausing sequence impairs targeting to the ER, thus leading to mislocalization (Yanagitani et al., 2011). The ubiquitinated population of VAPA gradually decreased during the CHX chase period without a significant loss of total VAPA proteins. The ubiquitinated VAPA was not destined for degradation, since cells treated with both CHX and MG132 did not accumulate ubiquitinated proteins (Fig. 4 B). By contrast, the ubiquitinated XBP1m was decreased during the CHX chase with the concomitant loss of total proteins. Both ubiquitinated and

total proteins of XBP1m were accumulated upon inhibiting the proteasome. This result suggests that VAPA exhibits features different from a typical misfolded protein despite having similar levels of ubiquitination (Fig. 4 B). Similarly, we observed that β-VAMP2 was gradually deubiquitinated upon inhibiting protein synthesis by CHX without a significant loss of total β-VAMP2 proteins (Fig. 4 C). Interestingly, the deubiquitination of monoubiquitinated and glycosylated β-VAMP2 was significantly slower than that of polyubiquitinated species (Fig. 4 C). This result also suggests that monoubiquitinated TA proteins can be inserted and glycosylated, whereas polyubiquitinated proteins are deubiquitinated before insertion into the ER membrane. We next asked whether complete deubiquitination of TA proteins can occur before their insertion into the ER membrane. To address this, we constructed a β-VAMP2-C_{KK} construct where all lysine residues in the cytosolic domain were replaced with arginine residues, leaving two lysine residues in the C-terminus after the TMD. We speculated that β-VAMP2-C_{KK} must be fully deubiquitinated before insertion, as the ubiquitination of C-terminal lysine residues would hinder the insertion of the TMD. Indeed, we detected very little monoubiquitinated and glycosylated β-VAMP2-C_{KK} compared with β-VAMP2 (Fig. 4 D). The monoubiquitinated and glycosylated band was sensitive to Endo H digestion, confirming that this population was inserted with monoubiquitination. These results support the conclusion that deubiquitination of TA proteins can occur either before or after insertion into the ER membrane.

We next asked whether TA protein ubiquitination in the cytosol is coupled with deubiquitination at the ER membrane. To test this, we monitored the newly synthesized TA proteins by chasing metabolically labeled cells expressing VAPA. The cells were fractionated at each time point to separate the cytosol from the membrane fraction. Immunoprecipitation of VAPA revealed a clear ubiquitination signal from VAPA in the cytosol at the zero time point (Fig. 4 E). Ubiquitinated VAPA in the cytosol fraction gradually disappeared during the chase period with a concomitant increase in the signal of inserted and glycosylated VAPA in the membrane fraction. We noticed that, although VAPA was inserted efficiently into the ER, as shown by its efficient membrane localization at 4 h (Fig. 4 E), VAPA was not fully glycosylated, likely due to a shorter C-terminal glycosylation motif compared with β-VAMP2 (Fig. S1 A). To further determine if TA protein deubiquitination occurs in vitro, we translated β-VAMP2 and stopped protein synthesis by removing ribosomes by centrifugation. The posttranslation incubation of ubiquitinated VAMP2 with crude rough microsomes prepared from HEK293 cells led to its insertion as shown by glycosylation with a concomitant reduction in ubiquitinated species (Fig. 4 F). Collectively, our results suggest that nascent TA proteins are ubiquitinated in the cytosol and yet are still routed to the ER membrane for deubiquitination and insertion.

ER-localized USP20 and USP33 deubiquitinate ER-targeted TA proteins

We next wanted to determine the mechanism by which ubiquitinated TA proteins are deubiquitinated at the ER membrane. Though most polyubiquitin chains are removed from TA proteins before insertion, as evidenced by the lack of simultaneously glycosylated and ubiquitinated TA proteins (Fig. S1 B), we hypothesized that an ER-localized DUB would be ideally positioned to target any ubiquitin still attached once a TA protein reaches the ER. We therefore focused on three DUBs—USP19, USP20, and USP33—that are known to associate with the ER membrane (Curcio-Morelli et al., 2003; Hassink et al., 2009; Thorne et al., 2011). To test if any of these ER-localized DUBs are involved in the deubiquitination of TA proteins, we generated CRISPR/Cas9-mediated HEK293 knockout cells of USP19, USP20, USP33, or a mitochondria-localized USP30 as a control (Fig. 5 A). Since USP20 and USP33 are homologous DUBs, we generated knockout cells depleted of both proteins as well. None of these DUBs affected the deubiquitination of VAPA when they were individually depleted in cells. By contrast, double knockout of homologous proteins USP20 and USP33 resulted in a significant accumulation of ubiquitinated VAPA compared with either WT or single knockout cells (Fig. 5 A). Consistent with previous studies (Thorne et al., 2011), we noticed that the depletion of USP20 increased the expression level of USP33 (Fig. 5 A), suggesting that these proteins play redundant functions in cells. Unlike USP19, which is anchored to the ER membrane via the C-terminal TMD (Hassink et al., 2009; Lee et al., 2014), USP20 and USP33 lack predictable TMDs. We therefore tested their membrane localization by cellular fractionation and immunoblotting. Both USP20 and USP33 are localized to the membrane fraction of semipermeabilized cells (Fig. 5 B). Additionally, immunoblotting of ER-derived microsomes revealed that USP20 and USP33 are localized at the ER membrane (Fig. 5 C). We further verified the ER localization of USP20 and USP33 via confocal microscopy. Endogenous USP33 colocalized with an ER protein calreticulin (Fig. 5 D). Consistent with our Western blot analysis, USP33 signal was elevated in USP20$^{-/-}$ cells compared with WT cells, whereas little to no signal was observed in USP33$^{-/-}$ cells (Fig. 5 D); however, endogenous USP20 was less readily detectable (Fig. S2 A). We therefore overexpressed USP20 and USP33 along with the ER control PDI (protein disulphide-isomerase) to verify their localization. Both USP20 and USP33 showed colocalization with PDI (Fig. 5 E).

Intriguingly, we observed the accumulation of ubiquitinated as well as glycosylated VAPA species in USP20/33$^{-/-}$ cells, which were confirmed by digestion with Endo H (Fig. 6 A). This result is consistent with our hypothesis that the ER-localized USP20/33 mediate deubiquitination after TA protein insertion and glycosylation in the ER membrane. Cellular fractionation further revealed that ubiquitinated VAPA was accumulated mostly in the membrane fraction of USP20/33$^{-/-}$ cells compared with WT cells, whereas the level of cytosolic VAPA ubiquitination was similar in both WT and USP20/33$^{-/-}$ cells (Fig. 6 B and Fig. S3 A). Interestingly, we only observed the accumulation of mono-, di-, and triubiquitinated species, but polyubiquitinated species were not significantly accumulated in the ER membrane of USP20/33$^{-/-}$ cells compared with WT cells (Fig. 6 B and Fig. S3 A). These results suggest that polyubiquitin chains are removed from TA proteins by a different DUB before insertion into the ER membrane.

Screening of TA substrates revealed that ubiquitinated species of mini-Otoferlin, βVAMP2, and Cb5 accumulate in USP20/

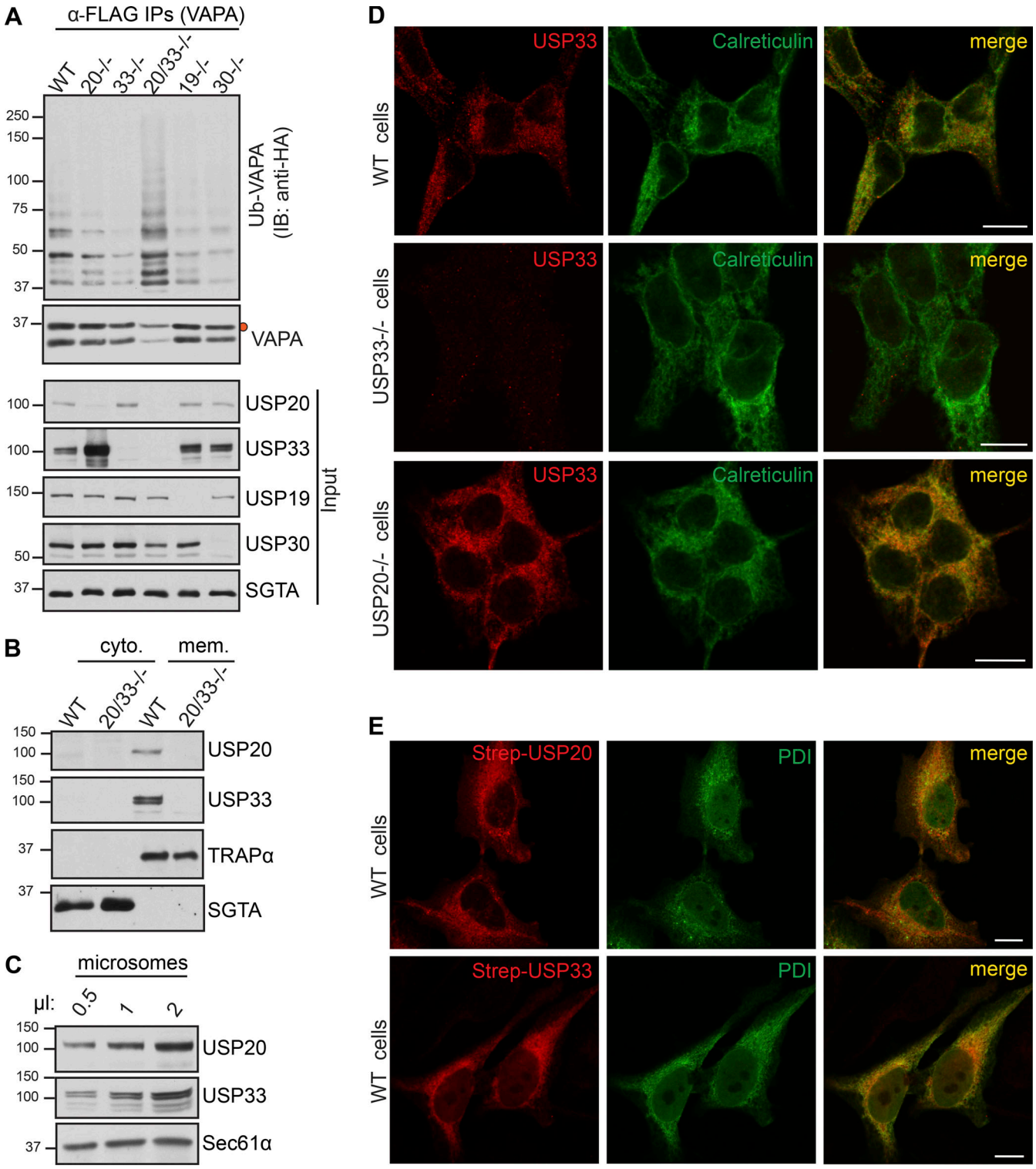

Figure 5. **ER-localized USP20 and USP33 are required for deubiquitination of TA proteins. (A)** HEK293 cells with the indicated CRISPR/Cas9 knockout cell lines were transfected with VAPA-FLAG and HA-ubiquitin. VAPA was immunoprecipitated (IP) and immunoblotted (IB) with anti-FLAG antibody for VAPA and anti-HA antibody for ubiquitinated (Ub) VAPA. The orange circle indicates the glycosylated form of VAPA. **(B)** WT HEK293 and USP20/33$^{-/-}$ cells were fractionated into cytosol (cyto.) and membrane (mem.) using 0.015% digitonin. Immunoblotting of TRAPα (membrane control) and SGTA (cytosolic control) shows the successful separation of the cytosol and membrane. Data are representative of two independent experiments. **(C)** Increasing amounts of rough microsomes isolated from HEK293 cells were immunoblotted for USP20, USP33, and the membrane protein Sec61α as a control. **(D)** WT, USP20$^{-/-}$, and USP33$^{-/-}$ HEK293 cells were stained for the indicated endogenous proteins. Confocal imaging shows colocalization signal (yellow) of USP33 (red) and calreticulin (green). Scale bar, 10 µm. Data are representative of two independent experiments. **(E)** HeLa cells were transfected with the ER control protein PDI and either USP20 or USP33 and then treated as in C for confocal microscopy. Scale bar, 10 µm.

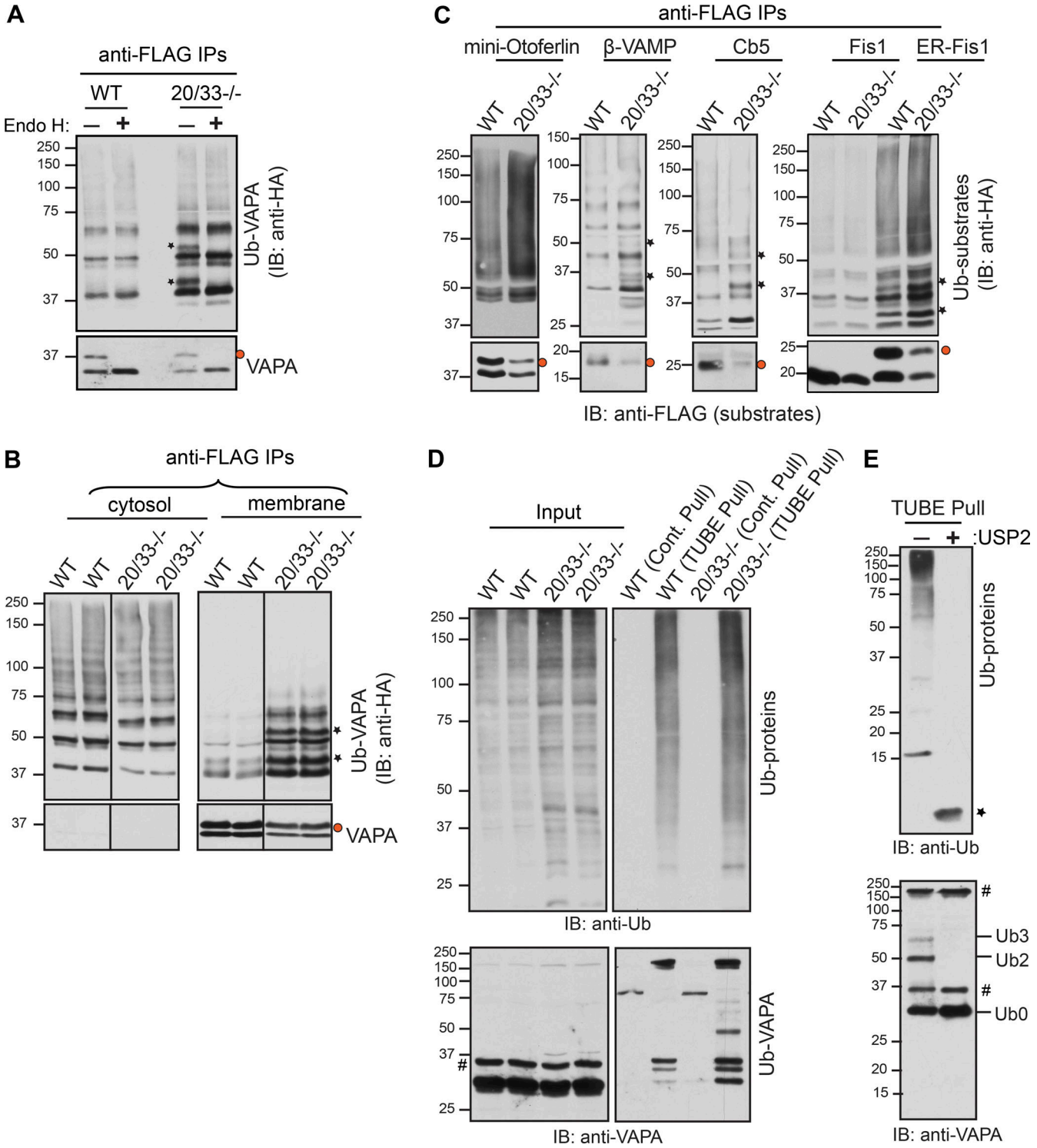

Figure 6. **Ubiquitinated TA proteins accumulate in USP20/33$^{-/-}$ cells. (A)** VAPA-FLAG and HA-ubiquitin were transfected into WT or USP20/33$^{-/-}$ HEK 293 cells. VAPA was immunoprecipitated (IP) and treated without or with Endo H for 6 h at 37°C. Samples were immunoblotted (IB) with anti-FLAG antibody for VAPA and anti-HA antibody for ubiquitinated (Ub) VAPA. The orange circle indicates the glycosylated form of VAPA, and the bands lost in the Endo H–treated sample, indicated by the star, represent ubiquitinated and glycosylated VAPA. **(B)** WT HEK293 and USP20/33$^{-/-}$ cells were fractionated into cytosol and membrane using 0.015% digitonin as in Fig. 5 A and analyzed by immunoblotting as in A. Note that nascent ubiquitinated TA proteins were hardly detected in the cytosol fraction by immunoblotting due to their low abundance, but they could be readily detected after metabolic labeling as shown in Fig. 1 E. **(C)** Cells expressing the indicated substrates along with HA-ubiquitin were examined as in A. **(D)** WT and USP20/33$^{-/-}$ cells were lysed with 1% Triton X-100 and endogenous ubiquitinated proteins were pulled down using TUBE agarose and analyzed by immunoblotting with anti-ubiquitin and anti-VAPA antibodies. The pound sign denotes an unknown band. **(E)** Samples were obtained from USP20/33$^{-/-}$ cells as in D and then TUBE agarose–bound endogenous ubiquitinated proteins were treated without or with USP2 before analyzing by immunoblotting. The pound sign denotes unknown bands, and the star indicates ubiquitin monomers.

33$^{-/-}$ cells, while mitochondria-localized Fis1 was unaffected (Fig. 6 C). We next wondered if artificially directing Fis1 to the ER membrane would force its deubiquitination to be dependent on USP20/33. To examine this, we constructed an ER-targeted Fis1 (ER-Fis1) in which the C-terminal tail is replaced with an N-glycosylation site (Fig. S1 A). Indeed, ubiquitinated as well as glycosylated ER-Fis1 was accumulated in USP20/33$^{-/-}$ cells relative to WT cells (Fig. 6 C), suggesting that the localization at the ER membrane is crucial for deubiquitination of TA proteins by USP20/33. Furthermore, we asked if the depletion of USP20/30 leads to the accumulation of endogenous ubiquitinated TA proteins. To test this, we isolated endogenous total ubiquitinated proteins from the total lysate of WT or USP20/33$^{-/-}$ cells using TUBEs (tandem-repeated ubiquitin-binding entities)–agarose. Immunoblotting with a ubiquitin antibody confirmed that TUBEs efficiently pulled down endogenous ubiquitinated proteins (Fig. 6 D). Importantly, we were able to detect endogenous ubiquitinated VAPA in WT cells and that the ubiquitinated VAPA accumulated more in USP20/33$^{-/-}$ cells (Fig. 6 D). Consistent with the results observed with our recombinant VAPA, USP20/33$^{-/-}$ showed the accumulation of mono- to triubiquitinated endogenous VAPA, which could be removed by USP2 (Fig. 6, D and E). We also noticed that unmodified VAPA was pulled down by TUBEs. This is presumably caused by an interaction between ubiquitinated and nonubiquitinated VAPA. The CHX and pulse-chase experiments revealed that the accumulated TA proteins with ubiquitin modifications in USP20/33$^{-/-}$ cells are not routed for proteasomal degradation (Fig. S3, A and B); however, the ubiquitinated XBP1m was degraded by proteasomes both in WT and USP20/33$^{-/-}$ cells (Fig. S3 B). Furthermore, we found no significant difference in the insertion of TA proteins between WT and USP20/33$^{-/-}$ cells (Fig. S3 C). Taken together, these results suggest that USP20/33 are responsible for the deubiquitination of TA proteins after their insertion into the ER membrane.

USP20 and USP33 play redundant roles in the deubiquitination of TA proteins

To determine whether both USP33 and USP20 are required for removing ubiquitin chains from TA proteins or if they play redundant roles, we complemented either USP33 or USP20 into USP20/33$^{-/-}$ cells and monitored the deubiquitination of VAPA by immunoblotting. Indeed, the complementation of either WT USP20 or USP33 completely deubiquitinated VAPA, supporting that either one is sufficient to remove ubiquitin chains from TA proteins (Fig. 7 A). We next asked if the catalytic activity of USP20 or USP33 is required for the deubiquitination of TA proteins. To address this, we generated catalytically inactive mutant versions of USP20 (C154S/H643Q) and USP33 (C194S/H665Q), as characterized by previous studies (Berthouze et al., 2009). Complementation with catalytically deficient mutants significantly increased the accumulation of ubiquitinated VAPA compared with cells expressing their WT counterparts (Fig. 7 A); therefore, the catalytic activity of USP20 or USP33 is essential for the deubiquitination of TA proteins. Interestingly, the expression of catalytically inactive mutants of USP20 and USP33 further increased the accumulation of ubiquitinated VAPA, suggesting that these mutants protect the ubiquitinated VAPA from other DUBs. Lastly, we wanted to determine if USP20 or USP33 was sufficient to remove ubiquitin chains from TA proteins. We therefore purified Strep-tagged USP20 or its catalytically inactive mutant (CH/SQ) from HEK293 cells (Fig. 7 B). We then immunoprecipitated radiolabeled nascent VAPA from the cytosol fraction of HEK293 cells expressing FLAG-tagged VAPA. The incubation of ubiquitinated VAPA with purified USP20 led to complete deubiquitination of VAPA, whereas the catalytically inactive USP20 mutant was not able to remove ubiquitin chains from VAPA (Fig. 7 C) Overall, these results establish that USP20 or USP33 directly removes the ubiquitin chains of TA proteins at the ER membrane.

Discussion

TA proteins are a vital class of membrane proteins that are posttranslationally targeted and inserted into cellular membranes (Borgese et al., 2019). Due to TA proteins' singular C-terminal hydrophobic TMDs, a critical challenge for them is to evade the cytosolic PQC, which normally recognizes exposed hydrophobicity (Ciechanover and Kwon, 2017; Fredrickson et al., 2013; Xu et al., 2016). In this study, we found that newly synthesized TA proteins are ubiquitinated in the cytosol. In contrast to the previously proposed model, ubiquitinated TA proteins are not destined for proteasomal degradation, but rather they are properly targeted, inserted, and deubiquitinated at the ER membrane. The ER-localized DUBs, USP20 and USP33, deubiquitinate TA proteins at the ER membrane (Fig. 8).

Both our in vitro and in vivo studies show that newly synthesized TA proteins are ubiquitinated in the cytosol. Our observation of TA protein ubiquitination is consistent with previous in vitro studies (Hessa et al., 2011; Shao et al., 2017). It was previously proposed that TA protein ubiquitination was due to the limitation of targeting chaperones in the cytosol; however, our in vitro and in vivo studies argue against this notion. Instead, TA proteins are ubiquitinated regardless of chaperone availability. Surprisingly, our data also suggest that ER-targeted TA proteins are ubiquitinated even in the absence of BAG6 in cells. This result suggests that TA proteins are ubiquitinated upstream of BAG6, likely as soon as their hydrophobic TMD is exposed to the cytosol after release from ribosomes. Our observation of BAG6-independent ubiquitination resembles the previous studies wherein BAG6 captures newly synthesized ubiquitinated proteins (Minami et al., 2010; Yau et al., 2017); however, we cannot rule out the possibility that another compensatory ubiquitination machinery is induced in BAG6$^{-/-}$ cells. An alternative possibility is that TA proteins are ubiquitinated twice, first after releasing from ribosomes and second by the BAG6 complex. This may explain why knockout of BAG6 did not significantly reduce the ubiquitination of TA proteins. Our data also do not rule out the ubiquitination of TA proteins occurring after binding to TRC40; however, this seems unlikely since TA substrate binding to TRC40 has been shown to be a commitment to ER targeting (Shao et al., 2017).

Previous in vitro reconstitution studies suggested that BAG6 functions as a triaging factor that either channels TA proteins to

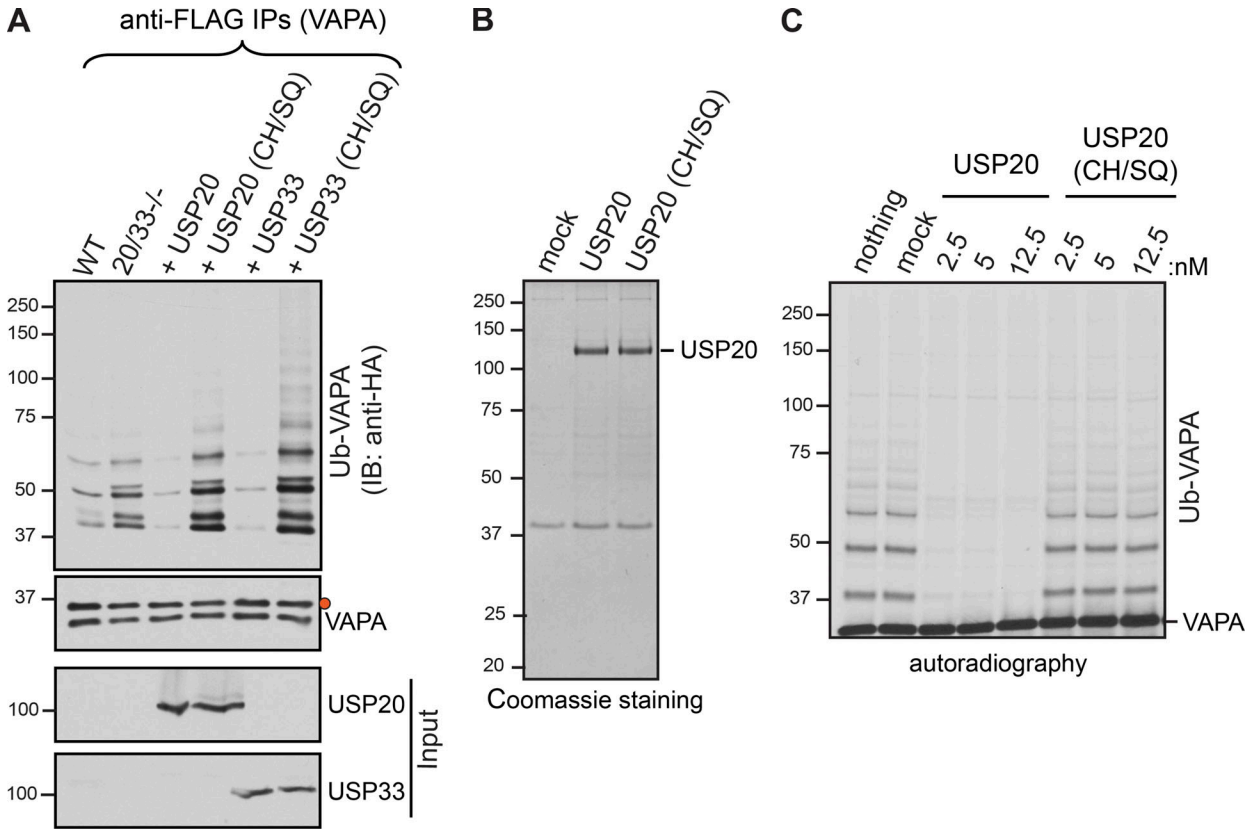

Figure 7. **The catalytic activity of USP20 or USP33 is required for the deubiquitination of TA proteins. (A)** USP20, catalytically inactive USP20 mutant (C154S and H643Q), USP33, or catalytically inactive USP33 mutant (C194S and H665Q) were transfected along with VAPA-FLAG and HA-ubiquitin. VAPA was immunoprecipitated (IP) via its FLAG tag and analyzed for ubiquitination (Ub) levels by immunoblotting (IB). The orange circle indicates the glycosylated form of VAPA. **(B)** A Coomassie-stained gel showing purified USP20 and USP20 mutant from HEK293 cells transiently overexpressing Strep-tagged versions of USP20. Nontransfected HEK293 cells were purified similarly and taken as a mock. **(C)** Radiolabeled VAPA was immunoprecipitated from the cytosol fraction of HEK293 cells expressing VAPA. The immunoprecipitated VAPA was treated with increasing amounts of purified USP20 or catalytically inactive USP20 mutant from B and analyzed by autoradiography. Data are representative of two independent experiments.

the targeting factor TRC40 for insertion or mediates ubiquitination of TA proteins for degradation when targeting fails (Shao et al., 2017). Several lines of our evidence suggest that ubiquitinated TA proteins are not destined for proteasomal degradation. First, ubiquitinated TA proteins are not accumulated in cells upon inhibiting the proteasome. Instead, they are deubiquitinated with almost no loss of total TA proteins. Second, ubiquitinated TA proteins can be passed off to endogenous TRC40 and inserted normally. Third, the deubiquitination of TA proteins is closely coupled with insertion at the ER membrane. Therefore, we propose that, despite being polyubiquitinated in the cytosol, TA proteins are properly targeted and inserted into membranes and deubiquitinated during this process.

Given that the ER membrane–localized TA proteins had little ubiquitin modification, we hypothesized that an ER-associated DUB may deubiquitinate TA proteins after insertion. Our CRISPR/Cas9 genetic screen of known ER-associated DUBs revealed that the depletion of USP20 and USP33 results in the accumulation of mono- to triubiquitinated and glycosylated TA proteins in the membrane with little effect on cytosolic polyubiquitinated TA proteins. This suggests that USP20/33 mainly act on ubiquitinated TA proteins after their insertion into the ER membrane, while other unidentified DUBs may remove the larger polyubiquitin chains from TA proteins before insertion. Additionally, our complementation experiment suggests that homologous USP20 and USP33 play redundant roles in removing ubiquitin chains from TA proteins. The precise mechanism by which USP20 and USP33 associate with the ER membrane remains to be investigated, since they lack TMDs, although previous studies have identified an amphipathic region that appears to be necessary for the ER membrane localization of USP33 (Thorne et al., 2011).

Surprisingly, we found that the ER-localized transmembrane DUB USP19 is dispensable for deubiquitination of ER-targeted TA proteins, despite the fact it can remove K48-linked ubiquitin chains (Lee et al., 2014). We speculate that the peripheral membrane association of USP20/33 may provide a unique advantage to access ubiquitin chains of TA proteins compared with USP19, which is anchored to the ER membrane via the C-terminal TMD. Since TA ubiquitination is dependent on the TMD, ubiquitination machinery targets lysine residues located proximal to the TMD (Rodrigo-Brenni et al., 2014). USP20/33 may be peripherally positioned to access the ubiquitin chains of TA proteins that are close to the lipid bilayer. This model is

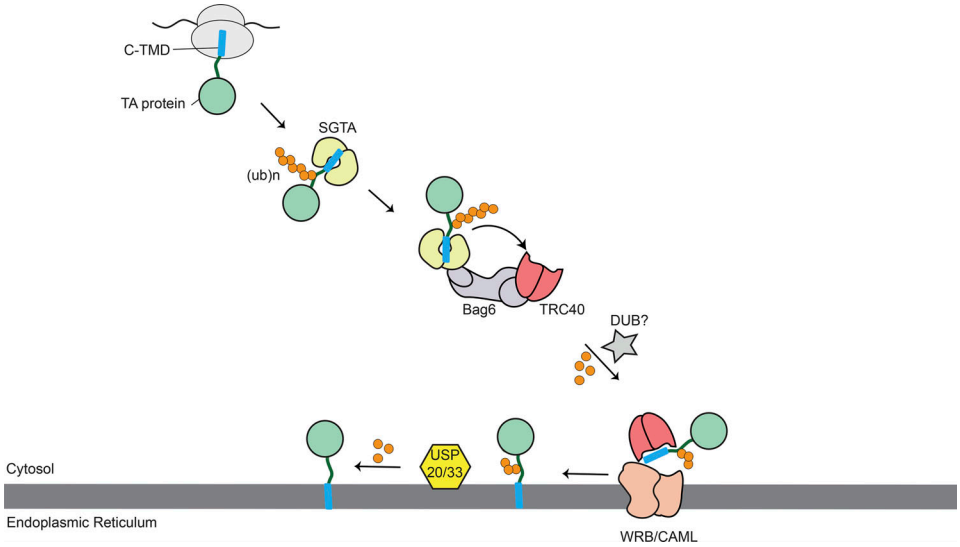

Figure 8. **Model of nascent TA protein ubiquitination and deubiquitination.** A fraction of newly synthesized TA proteins is polyubiquitinated in the cytosol. The polyubiquitinated TA proteins are captured by TRC40, likely with the help of SGTA and the BAG6 complex. The polyubiquitinated TA proteins are partially deubiquitinated by an unknown cytosolic DUB before insertion into the ER membrane. ER membrane–associated USP20 and USP33 deubiquitinate the remaining one to three ubiquitin modifications on TA proteins.

consistent with the recent findings that USP20 can remove ubiquitin chains from a lysine residue of HMGCR (3-hydroxy-3-methyl-glutaryl–coenzyme A reductase) that is located close to the lipid bilayer (Lu et al., 2020). Since USP20/33 removes ubiquitin chains of TA proteins that use either the TRC40 or ER membrane protein complex pathwayfor insertion into the ER membrane (Guna et al., 2018), deubiquitination of TA proteins by USP20/33 may not be directly coupled with insertion. We envision that USP20 and USP33 may also function as general ER surveillance factors to remove ubiquitin chains from membrane proteins that are promiscuously ubiquitinated by ER-bound E3 ligases (Zhang et al., 2013), thereby rescuing functional membrane proteins from ERAD (ER-associated protein degradation).

It is unclear why ubiquitinated TA proteins that accumulate in USP20/33-depleted cells are not routed for proteasomal degradation. One explanation for this observation is that these TA proteins consist of mono-, di-, and triubiquitinated species that are likely not suitable for the p97 ATPase-mediated extraction from the ER membrane for degradation by cytosolic proteasomes (Bodnar and Rapoport, 2017). However, we predict that these modifications could inhibit the function of a TA protein by occluding interaction with partner proteins. We found that USP20/33-mediated removal of ubiquitin chains from TA proteins is not a prerequisite for insertion into the ER membrane; however, future studies using various TA proteins, including ones containing lysine residues succeeding the C-terminal TMD, are needed to determine if deubiquitination is required for the insertion of select TA substrates. Our results suggest that USP20/33 are not absolutely essential for deubiquitinating TA proteins, as deubiquitination is reduced but not completely blocked in USP20/33$^{-/-}$ cells. This observation implies that other cytosolic or ER-associated DUBs can partially compensate for the role performed by USP20/33.

Our quantification result suggests that only a small amount (8%) of the cytosolic nascent TA protein is ubiquitinated in the cytosol fraction. However, we predict that this number is an underestimate because ubiquitin modifications on TA proteins may survive only a short period, as they are counteracted by cytosolic DUBs. This notion is supported by our observation that the mislocalized XBP1m, which carries similar levels of ubiquitination as VAPA, is rapidly recognized for proteasomal degradation. We speculate that TA proteins are not accidentally ubiquitinated by the cytosolic PQC and that ubiquitination may play important roles in the biogenesis of TA proteins. One intriguing function for TA protein ubiquitination could be the suppression of TA protein activity until it reaches the target destination in the cell. This may be particularly important for TA proteins that interact with proteins from other cellular membranes.

We have shown that ER-targeted TA proteins are ubiquitinated in the cytosol and subsequently deubiquitinated and inserted. We propose that such ubiquitination of nascent membrane proteins and the subsequent deubiquitination at the target membrane may be common for all posttranslationally inserted membrane proteins. Whether targeted to the mitochondria, peroxisomes, or lipid droplets, posttranslationally inserted membrane proteins face similar challenges in traversing the aqueous cytosol with their hydrophobic domains. This idea is consistent with the recent findings that USP30 deubiquitinates mitochondrial proteins that are imported through the translocase of outer membrane complex (Ordureau et al., 2020; Phu et al., 2020). However, it remains to be determined if USP30 can deubiquitinate mitochondrial-targeted TA proteins.

Materials and methods

DNA constructs

pcDNA 3.1 (Thermo Fisher Scientific) or pCDNA5/FRT/TO (Invitrogen) vectors were used for mammalian expression. To

construct TA model substrates, PCR amplification of the gene in question was performed with Phusion high-fidelity DNA polymerase (Thermo Fisher Scientific). A FLAG tag (MDYKDDDDK) was added to the N-terminal primers. For ER-targeted TA proteins, an opsin tag was added to the C-terminal primers as seen in Fig. S1 A. Restriction enzyme cut sites were also added to the primers to allow for digestion (restriction enzymes from New England Biolabs) followed by ligation by T4 DNA Ligase (New England Biolabs) into the vectors above. For VAPA ΔTMD, the amino acids from 227 to 249 were deleted using phosphorylated primers with the Phusion site-directed mutagenesis protocol (Thermo Fisher Scientific). DHFR was a gift from Dr. Zai-Rong Zhang (University of Chinese Academy of Sciences, Shijingshan District, Beijing, China) and cloned into the pCDNA5/FRT/TO as above. For DHFR-VAMP-TMD, human VAMP2 TMD (aa 91–114) was PCR amplified and inserted into the C-terminus of DHFR using a standard cloning procedure. β-VAMP2 containing the cytosolic domain of SEC61β and the TMD of VAMP2 was previously described (Mariappan et al., 2010). β-VAMP2 with lysine mutations was generated using Pfu polymerase (Agilent Technologies)-based site-directed mutagenesis. To construct SEC61β–hydrophobic VAMP2 TMD (β-VAMP2-Hy), the indicated amino acids in Fig. S1 A were replaced by site-directed mutagenesis. Zebrafish mini-Otoferlin containing amino acids from 1495 to 1773 was gifted from Dr. Erdem Karatekin (Nanobiology Institute, Yale University, West Haven, CT) and cloned into pCDNA5/FRT/TO with a FLAG and opsin tag as above. Rabbit Cb5 was gifted from the Hegde laboratory (MRC Laboratory of Molecular Biology, Cambridge, UK) and cloned into the pCDNA5/FRT/TO as above with the addition of an N-terminal FLAG tag and a C-terminal opsin tag. FLAG-HA-USP20 (Addgene; #22573) and FLAG-HA-USP33 (Addgene; #22601) were a gift from Wade Harper (Department of Cell Biology, Blavatnik Institute, Harvard Medical School, Boston, MA). USP20 and USP33 were cloned into the pCDNA5/FRT/TO as above with the addition of the N-terminal His-Strep-TEV sequence (MHHHHHHASGGWSHPQFEKASENLYFQGVDGT). Two rounds of site-directed mutagenesis were used to create catalytically inactive USP20 (C154S/H643Q) and USP33 (C194S and H665Q) using Pfu polymerase. FLAG-XBP1u (Plumb et al., 2015) was used as a template to create the XBP1u mutant (L246A) using site-directed mutagenesis. PDI-FLAG (Addgene; #31382) was gift from David Ron (Cambridge Institute for Medical Research, University of Cambridge, Cambridge, UK). The coding sequences of all constructs were verified by sequencing (Yale Keck DNA Sequencing Facility).

Antibodies and reagents

Antibodies used for immunoblotting are as follows: mouse α-HA-HRP (Cell Signaling Technology; #2999S); rat α-FLAG L5 (BioLegend; #12775); and rabbit α-FLAG, rabbit α-GFP, rabbit α-RFP, rabbit α-TRAPα, and rabbit α-Sec61α are a gift from Dr. Ramanujan Hegde (MRC Laboratory of Molecular Biology, Cambridge, UK). Rabbit α-SGTA, rabbit α-BAG6, and rabbit α-TRC40 have been previously described (Mariappan et al., 2010; Shao et al., 2017). Mouse α-CAML (Origene; #TA504363), rabbit α-USP19 (Invitrogen; #PA5-97239), mouse α-USP30 (Santa Cruz Biotechnology; #sc-515235), mouse α-tubulin (Abcam; #ab7291), goat α-rat-HRP (Cell Signaling Technology; #7077), goat α-mouse-HRP (Jackson ImmunoResearch; #115-035-003), goat α-rabbit-HRP (Jackson ImmunoResearch; #111-035-003), goat α-rabbit IgG-Cy3 (Jackson ImmunoResearch; #111–165-003), goat α-mouse IgG-Cy2 (Jackson ImmunoResearch; #115–225-166), goat α-rabbit IgG-Cy2 (Jackson ImmunoResearch; #111–225-144), goat α-rat IgG-Cy2 (Jackson ImmunoResearch; #112–225-167), goat α-mouse IgG-Alexa 657 (Invitrogen; #A-21235) or goat α-rabbit IgG-Alexa 647 (Invitrogen; #A27040), rabbit α-USP20 (Proteintech; #17491-1-AP), rabbit α-USP33 (Proteintech; #20445-1-AP), mouse α-USP33 (Sigma-Aldrich; WH0023032M1), rabbit α-calreticulin (Affinity BioReagents; #PA3-900), mouse α-PDI (Affinity BioReagents; #MA3-018), mouse α-ubiquitin (Enzo Life Sciences; #ADI-SPA-203-F), and rabbit α-K48 linkage–specific polyubiquitin (Cell Signaling Technology; #8081S), and rabbit α-VAPA (Proteintech; #15275-1-AP). His-ubiquitin (#U-530), USP2 (#E-506), and USP30 (#E-582) purified proteins and TUBE agarose (#AM-130) were purchased from Boston Biochem. Detergents were purchased as follows: digitonin (EMD Millipore), Triton X-100 (Thermo Fisher Scientific), sodium deoxycholate (Sigma-Aldrich), and SDS (Sigma-Aldrich), saponin (Sigma-Aldrich), 37% formaldehyde (Avantor), Hoechst 33342 stain (Cell Signaling Technology; #4082S), and Tween 20 (American Bioanalytical).

In vitro translation and ubiquitination

In vitro transcription and translation were performed using the previous protocols with the following modifications (Mariappan et al., 2010; Sharma et al., 2010). For in vitro transcription reactions, PCR products encoding N-terminally FLAG-tagged TA proteins were used as templates. The PCR products were amplified from either pCDNA 3.1 or pCDNA5/FRT/TO TA protein constructs using the 5′ primer that includes the Sp6 promoter sequence and anneals to the CMV promoter and the 3′ primer that anneals to the poly(A) tail. In vitro transcription was performed using SP6 polymerase (New England Biolabs) and RNase Inhibitor (Promega) at 40°C for 1.5 h. The transcription reaction products were directly added to in vitro translation reactions containing a mixture of hemin, nuclease-treated RRL, S35 methionine (PerkinElmer; #NEG009T005MC), and 10 µM His-tagged ubiquitin (Boston Biochem), and were incubated for 40 min at 32°C. In some reactions, recombinant zebrafish TRC40, purified from *Escherichia coli* as described previously (Mariappan et al., 2010), was included during translations. The translation was terminated by either adding 1 mM puromycin or removing ribosomes by centrifugation at 70,000 rpm in the TLA 120.1 rotor for 30 min. 2 µl of crude microsomes prepared from HEK293 cells as described in Sundaram et al. (2017) was added to 20 µl translation reactions and further incubated for 30 min at 32°C. The reactions were diluted to 0.1% SDS with the Triton buffer (50 mM Tris-HCl, 1% Triton X-100, and 150 mM NaCl) and incubated with either 20 µl Talon beads to capture ubiquitin-conjugated TA proteins or 12 µl anti-FLAG beads (BioLegend) to capture FLAG-tagged TA proteins. After incubation for 1.5 h at 4°C, beads were washed three times with 1 ml Triton

buffer and eluted with 50 µl of 2× SDS sample buffer by boiling for 5 min at 95°C. The eluted samples were resolved in either 7.5% Tris-Tricine gel for ubiquitin-conjugated TA proteins or 10% Tris-Tricine gel for total TA proteins and processed for autoradiography.

Cell culture and generating knockout cells using CRISPR/Cas9

HEK293- Flp-In, T-REx 293, and HeLa T-REx (Thermo Fisher Scientific), and HEK293T cell lines were cultured with high-glucose DMEM (Corning), 10% FBS (Gibco), 100 U/ml penicillin, and 100 mg/ml streptomycin (Gibco) at 37°C and 5% CO_2. HEK293-Flp-In T-Rex cells were used for generating SGTA$^{-/-}$, BAG6$^{-/-}$ cells, USP19$^{-/-}$, USP30$^{-/-}$, USP20$^{-/-}$, USP33$^{-/-}$, and USP20/33$^{-/-}$, while HEK293T cells were used for making the partial knockout of CAML. The knockout cell lines were generated using the CRISPR/Cas9 system as previously described (Mali et al., 2013; Ran et al., 2013). Cells were transfected with pSpCas9(BB)-2A-Puro and gRNA expression plasmid targeting SGTA (targeting sequence: 5′-CTTGTATGTCTCGTTGTCG-3′), BAG6 (targeting sequence: 5′-CCATACCGAGGTGGCGGTC-3′), CAML (targeting sequence: 5′-TGGCCGTCGCTACCGACGG-3′), USP30 (targeting sequence: 5′-CGCTCATCTTCCAATGACG-3′), USP19 (targeting sequence: 5′-GAGCAAGGATGGAGATCCT-3′), USP20 (targeting sequence: 5′-GAGGTTCTTCATGCCCGTG-3′), or USP33 (targeting sequence: 5′-GCGAAGCATATGCTCCACA-3′). The transfected cells were grown for 24 h and treated with 2.5 µg/ml puromycin for 72 h to select the successfully transfected clones. Single-cell clones were isolated by plating at 0.5 cells/well in 96-well plates. All knockouts were confirmed by immunoblotting. For generating knockout of both USP20 and USP33, pSpCas9(BB)-2A-Puro (Addgene; #62988) was cotransfected with USP20 and USP33 gRNAs and followed the procedure as outlined above. For Fig. S1 C, HEK293T cells were transfected with pcDNA 3.1/FLAG-β-VAMP2. Cells stably expressing β-VAMP2 were selected by treating with zeocin (300 µg/ml) for 3 wk. The individual clones were manually picked, and the expression of the β-VAMP2 was analyzed by immunoblotting.

Immunoprecipitation of ubiquitinated TA proteins from cells

To examine the polyubiquitination of TA proteins, HEK293 cells (0.75 × 10^6/well) were plated on polylysine-coated (0.15 mg/ml) six-well plates and transiently transfected with 0.75 µg pCDNA3/HA-ubiquitin plasmid, 1.25 µg of indicated TA constructs, and 5 µl Lipofectamine 2000 (Invitrogen) mixed in Opti-MEM (Gibco). 24 h after transfection, cells were harvested in radioimmunoprecipitation assay buffer (RIPA) buffer containing 50 mM Tris-HCl, pH 8.0, 150 mM NaCl, 0.1% SDS, 0.5% sodium deoxycholate (Millipore Sigma), 1× cOmplete protease inhibitor cocktail (Millipore Sigma), 1 mM EDTA (American Bioanalytical), and 2 mM N-ethylmaleimide (NEM; Sigma-Aldrich). After centrifugation at 20,000 *g* for 10 min, lysates were incubated with rat anti-FLAG beads (BioLegend) for 1.5 h. The beads were then washed with 1 ml RIPA buffer three times. Washed beads were directly boiled with 50 µl 2× SDS sample buffer for 5 min followed by immunoblotting with anti-HA for ubiquitin-modified TA proteins and anti-FLAG antibodies for TA proteins.

In some experiments, cells were treated with 200 µg/ml CHX, 20 µM MG132, or both, as indicated in the figure legends, before harvesting the cells with RIPA buffer. In some experiments, transfected cells were rinsed on a plate with 1× PBS and then incubated for 10 min at 4°C in 0.5 ml of 50 mM Hepes, 150 mM NaCl, 0.01% digitonin, 2 mM NEM, and 1× cOmplete protease inhibitor cocktail. This served as the cytosolic fraction. Cells were rinsed once with the same buffer to further remove cytosolic proteins and then scraped off the plate using 1 ml RIPA buffer for a crude membrane fraction. Samples were centrifuged to remove cellular debris, and the cytosolic fraction was made up to 1 ml using RIPA buffer. The two fractions were immunoprecipitated as above. For the endogenous TRC40 immunoprecipitation shown in Fig. 3, E and F, the cells were harvested in 1× PBS and centrifuged at 10,000 *g* for 2 min. Cell pellets were lysed with 1 ml of lysis buffer (50 mM Tris-HCl, pH 7.4, 150 mM NaCl, and 0.05% digitonin, 2 mM NEM, and 1× protease inhibitor) and brief vortexing. The samples were centrifuged at 20,000 *g* for 10 min and the pellets were discarded. Samples were either incubated with anti-TRC40 antibodies or anti-GFP antibodies for 1.5 h at 4°C. The antibodies were recovered using Protein A agarose (RepliGen) for 1 h at 4°C. The beads were washed three times with 1 ml of lysis buffer without protease inhibitor or NEM. Washed beads were resuspended in 50 µl SDS sample buffer, boiled for 5 min at 95°C, and analyzed by immunoblotting for the indicated antigens in the figure legends.

Metabolic labeling and immunoprecipitation

HEK293 cells (0.75 × 10^6/well) were plated on polylysine-coated (0.15mg/ml) six-well plates and transiently transfected with 2 µg of indicated plasmids using 5 µl Lipofectamine 2000 (Invitrogen). For metabolic labeling, cells were incubated in cysteine- and methionine-free media with 10% dialyzed FBS for 30 min. Then, cells were labeled with 80 µCi/ml Express35S Protein Labeling Mix (PerkinElmer; #NEG072014MC) for 30 min, unless otherwise indicated in the figure legends. Cells were rinsed with 1× PBS and chased with complete DMEM medium supplemented with 2 mM methionine and 2 mM cysteine. The labeled cells were directly harvested in 1 ml RIPA buffer for Figs. 1 G and 4 A and immunoprecipitated using anti-FLAG beads. For Figs. 1 E, 4 E, 6 C, and S2 A, labeled cells were permeabilized with 0.01% to 0.015% digitonin and fractionated into cytosol and membrane fractions, as described above, and immunoprecipitated using anti-FLAG beads. The immunoprecipitants were analyzed by SDS-PAGE autoradiography.

Isolation of endogenous ubiquitinated proteins

Endogenous TRC40-interacting proteins were purified for Fig. 3 G by harvesting 2 × 15-cm plates of HEK293 cytosol via the digitonin buffer (50 mM Tris-HCl, pH 7.4, 150 mM NaCl, and 0.015% digitonin, 2 mM NEM, and 1× protease inhibitor). The cytosol samples were incubated with ∼100 µl of protein A agarose beads conjugated to either rabbit α-TRC40 or control rabbit α-RFP antibodies for 1.5 h at 4°C. Beads were thoroughly washed five times in 0.015% digitonin. Then, 800 µl Triton X-100 buffer (50 mM Tris-HCl, pH 7.4, 150 mM NaCl, and 1% Triton X-100) was used to elute proteins bound to TRC40 via hydrophobic interactions. The elutions were precipitated using trichloroacetic acid and solubilized in 2× SDS sample buffer. For Fig. 6 D,

one 15-cm plate of either confluent HEK293 or USP20/33$^{-/-}$ cells were harvested and lysed with 1 ml of lysis buffer (50 mM Tris-HCl, pH 7.4, 200 mM NaCl, and 1% Triton X-100, 2 mM NEM, 10 mM iodoacetic acid, and 1× protease inhibitor). After centrifugation at 20,000 *g* for 20 min at 4°C, the supernatant was incubated with either 40 µl slurry of Strep-Tactin agarose (IBA) as a control or TUBE agarose (Boston Biochem) for 1.5 h at 4°C. The beads were washed three times with 1 ml of 50 mM Tris-HCl, pH 7.4, 200 mM NaCl, and 1% Triton X-100. Bound proteins were boiled in 60 µl of 2× SDS sample buffer and analyzed by immunoblotting.

Purification of recombinant USP20

5 million HEK293 cells were plated on a polylysine-coated (0.15 mg/ml) 10-cm plate and transiently transfected with 12 µg of either His-Strep USP20 or USP20 (CH/SQ) plasmid using 72 µl of polyethylenimine (Polysciences; a gift from Dr. Fabian Giska, Gupta Lab, Nanobiology Institute, Yale University, West Haven, CT). After 48 h of transfection, cells were harvested and lysed with 1 ml of lysis buffer (50 mM Tris-HCl, pH 7.4, 200 mM NaCl, 0.5% Triton X-100, and 1× protease inhibitor). After centrifugation at 20,000 *g* for 20 min, the supernatant was incubated with 200 µl of Strep-Tactin-XT beads (IBA) for 30 min at 37°C. The beads were washed five times with 1 ml lysis buffer without protease inhibitor on a 2-ml column. Bound proteins were incubated with 200 µl lysis buffer containing 50 mM Biotin for 5 min and eluted using gravity flow. The elutions were repeated two more times and analyzed along with BSA by Coomassie blue staining. The proteins were quantified using ImageJ relative to a known concentration of BSA.

Deubiquitinase and Endo H treatments

The Endo H digestions for Figs. 4 D, 6 A, and S1 A were performed after the indicated proteins were immunoprecipitated and boiled in SDS buffer for 5 min. The eluted samples were mixed with an equal volume of 1× Glycobuffer 5 (New England Biolabs) supplemented with 2% Triton X-100 and incubated without or with Endo H for 6 h at 37°C. The reactions were directly boiled with an equal volume of 3× SDS sample buffer and analyzed by immunoblotting. For Fig. 3 G, the elution from the α-TRC40 beads was split into two equal parts. One aliquot was kept on ice and the other was incubated with 138 nM of USP2 with shaking at 37°C for 2 h and then TCA precipitated as described above. For Fig. 5 H, TUBE agarose bound endogenous ubiquitinated were prepared for Fig. 6 E, as above. A final wash was performed with 1 ml DUB buffer (50 mM Tris-HCl, pH 7.4, 50 mM NaCl, 10% glycerol, 5 mM DTT, and 0.1% Triton X-100). The beads were then incubated with 200 nM USP2 with shaking at 37°C for 2 h. The reactions were then adjusted to 2× SDS sample buffer and boiled for 5 min before analyzing by immunoblotting. For Fig. S1 H, VAPA was immunoprecipitated from the cytosol fraction using α-FLAG beads. Before boiling, the immunoprecipitants were washed once with DUB buffer and treated with 200 nM USP2 or USP30 catalytic domain as indicated for 2 h at 37°C with shaking. The reactions were then adjusted to 2× SDS sample and boiled before analyzing by autoradiography. For Fig. 6 C, immunoprecipitated VAPA from the cytosol fraction was incubated with the increasing concentration of either purified WT USP20 or USP20 (CH/SQ) for 35 min at 37°C with shaking. The reactions were terminated by boiling with 2× SDS sample buffer and analyzed by autoradiography.

Immunoblotting

Samples were run on either 10% or 7.5% acrylamide Tris-Tricine SDS-PAGE gels at 100 V for 1.5 h. Proteins from the gels were transferred onto nitrocellulose membranes (Bio-Rad) using 100 V for 1 h. Membranes were then blocked in 1× PBS/0.1% Tween 20 (PBST) containing 5% milk (American Bioanalytical) for 45 min. The primary antibodies were diluted in 5% BSA (Millipore Sigma) and incubated with the membranes for 1.5 h at ambient temperature. Membranes were washed five times with PBST for 5 min per wash. The secondary antibody conjugated with HRP was incubated for 1 h in 5% milk and washed as above before developing with ECL. To detect HA-ubiquitin–conjugated TA proteins, the membranes were incubated with rabbit anti–HA-HRP antibody (Cell Signaling Technology) prepared in 5% BSA/PBST for 3 h at 4°C. The antibody can be stored at −20°C and used multiple times. After a final wash cycle, membranes were blotted dry and incubated in Perce ECL Western Blotting Substrate, SuperSignal West Pico, or Femto Substrate (Thermo Fisher Scientific) for 4 min and finally exposed onto HyBlot autoradiography films (Denville). The program ImageJ (National Institutes of Health) was used to quantify the intensity of bands from the films.

Microscopy

HEK293-Flp-In T-REx 293 WT, USP20$^{-/-}$, or USP33$^{-/-}$ cells were grown on polylysine-coated glass microscope slides. The cells were rinsed once with PBS and then fixed for 5 min with 3.7% formaldehyde in PBS. The fixed cells were rinsed twice with PBS and then permeabilized with 0.1% Triton X-100 in PBS. Cells were rinsed twice in PBS with 10% FBS and 0.01% saponin and then blocked for 1 h in PBS/FBS/saponin. HEK cells were incubated for 1 h with 1:100 dilution of mouse α-USP33 and rabbit α-calreticulin or rabbit α-USP20 and mouse α-PDI in PBS/FBS/saponin. Cells were washed five times for 5 min per wash. Cells were stained with a combination of goat α-mouse IgG-Cy2 (Jackson ImmunoResearch; #115–225-166) and goat α-rabbit IgG-Cy3 (Jackson ImmunoResearch; #111–165-003) for USP33/calreticulin or goat α-rabbit IgG-Cy2 (Jackson ImmunoResearch; #111–225-144) and goat α-mouse IgG-Cy3 (Jackson ImmunoResearch; #115–165-003) for USP20/PDI at 1:100 dilution in PBS/FBS/saponin all while covered to protect the fluorophores from excess light. The cells were washed five times again. Cells were rinsed once with PBS, and nuclei were stained using Hoechst 33342 stain (Cell Signaling Technology; #4082S) in PBS for 15 min. Cells were washed five times with PBS, and the coverslips were mounted onto slides with Fluoromount G (SouthernBiotech; #0100-01). The mounting was allowed to set overnight at 4°C while covered. HeLa T-REx cells were treated similarly as above with a few changes. Strep-USP33 or Strep-USP20 was transfected along with the ER control PDI-FLAG into cells by Lipofectamine 2000 (Invitrogen). Rat α-FLAG and either mouse α-USP33 or rabbit α-USP20 were used as primaries

followed by staining with goat α-RAT IgG-Cy2 (Jackson ImmunoResearch; #112–225-167) and either goat α-mouse IgG-Alexa657 (Invitrogen; #A-21235) or goat α-rabbit IgG-Alexa 647 (Invitrogen; #A27040). Confocal microscopy was performed on the slides using the Leica SP8 DMI6000 Confocal Microscope with a 63× oil objective, 1.40 aperture, and a PMT (photomultiplier tube) detector. Lasers at 405-, 488-, 561-, and 633-nm wavelengths were used to excite the Hoechst, Cy2, Cy3, and Alexa 647, respectively. Leica's LAS X software was used to capture and edit the gain, contrast, color, and scale bars of the images.

Online supplemental material

Fig. S1 shows the characterization of TA protein ubiquitination. Fig. S2 shows the endogenous USP20 localization. Fig. S3 shows the accumulation of ubiquitinated TA proteins in cells lacking USP20/33.

Acknowledgments

We are grateful to Mariappan Lab members Sha Sun, Xia Li, and Matthew Jordan for fruitful discussions, help with experiments, and comments on the manuscript. We thank Dr. Yihong Ye (Laboratory of Molecular Biology, National Institute of Diabetes and Digestive and Kidney Diseases, National Institutes of Health, Bethesda, MD) for providing HEK293T USP19$^{-/-}$ cells. We are grateful to Dr. Ramanujan Hegde for various antibodies and plasmids. We thank Dr. Robert Keenan (Department of Biochemistry and Molecular Biology, The University of Chicago, Chicago, IL) for purified TRC40. We thank Suhila Appathurai for making HEK293 BAG6$^{-/-}$ cells and Zhouping Hong for creating HEK293 SGTA$^{-/-}$ cells. We thank Dr. Zai-Rong Zhang for the DHFR plasmid. We thank Dr. Erdem Karatekin for the mini-Otoferlin construct. We thank Dr. James Rothman for use of the Leica Confocal Microscope.

This work is funded by National Institutes of Health grants R01GM117386 and R21AG056800 (both to M. Mariappan). J.A. Culver was supported by National Institutes of Health Cellular, Biochemical, and Molecular Sciences training grant T32 637 GM007223.

The authors declare no competing financial interests.

Author contributions: J.A. Culver designed and performed most of the experiments with help from M. Mariappan. M. Mariappan conceived and supervised the project. J.A. Culver and M. Mariappan wrote the manuscript.

Submitted: 12 April 2020
Revised: 19 December 2020
Accepted: 24 February 2021

References

Aviram, N., T. Ast, E.A. Costa, E.C. Arakel, S.G. Chuartzman, C.H. Jan, S. Haßdenteufel, J. Dudek, M. Jung, S. Schorr, et al. 2016. The SND proteins constitute an alternative targeting route to the endoplasmic reticulum. *Nature.* 540:134–138. https://doi.org/10.1038/nature20169

Berthouze, M., V. Venkataramanan, Y. Li, and S.K. Shenoy. 2009. The deubiquitinases USP33 and USP20 coordinate beta2 adrenergic receptor recycling and resensitization. *EMBO J.* 28:1684–1696. https://doi.org/10.1038/emboj.2009.128

Bodnar, N.O., and T.A. Rapoport. 2017. Molecular Mechanism of Substrate Processing by the Cdc48 ATPase Complex. *Cell.* 169:722–735.e9. https://doi.org/10.1016/j.cell.2017.04.020

Borgese, N., J. Coy-Vergara, S.F. Colombo, and B. Schwappach. 2019. The Ways of Tails: the GET Pathway and more. *Protein J.* 38:289–305. https://doi.org/10.1007/s10930-019-09845-4

Chacinska, A., C.M. Koehler, D. Milenkovic, T. Lithgow, and N. Pfanner. 2009. Importing mitochondrial proteins: machineries and mechanisms. *Cell.* 138:628–644. https://doi.org/10.1016/j.cell.2009.08.005

Chartron, J.W., W.M. Clemons Jr., and C.J. Suloway. 2012. The complex process of GETting tail-anchored membrane proteins to the ER. *Curr. Opin. Struct. Biol.* 22:217–224. https://doi.org/10.1016/j.sbi.2012.03.001

Chio, U.S., H. Cho, and S.O. Shan. 2017. Mechanisms of Tail-Anchored Membrane Protein Targeting and Insertion. *Annu. Rev. Cell Dev. Biol.* 33:417–438. https://doi.org/10.1146/annurev-cellbio-100616-060839

Ciechanover, A., and Y.T. Kwon. 2017. Protein Quality Control by Molecular Chaperones in Neurodegeneration. *Front. Neurosci.* 11:185. https://doi.org/10.3389/fnins.2017.00185

Colombo, S.F., R. Longhi, and N. Borgese. 2009. The role of cytosolic proteins in the insertion of tail-anchored proteins into phospholipid bilayers. *J. Cell Sci.* 122:2383–2392. https://doi.org/10.1242/jcs.049460

Curcio-Morelli, C., A.M. Zavacki, M. Christofollete, B. Gereben, B.C. de Freitas, J.W. Harney, Z. Li, G. Wu, and A.C. Bianco. 2003. Deubiquitination of type 2 iodothyronine deiodinase by von Hippel-Lindau protein-interacting deubiquitinating enzymes regulates thyroid hormone activation. *J. Clin. Invest.* 112:189–196. https://doi.org/10.1172/JCI18348

Cymer, F., G. von Heijne, and S.H. White. 2015. Mechanisms of integral membrane protein insertion and folding. *J. Mol. Biol.* 427:999–1022. https://doi.org/10.1016/j.jmb.2014.09.014

Denic, V., V. Dötsch, and I. Sinning. 2013. Endoplasmic reticulum targeting and insertion of tail-anchored membrane proteins by the GET pathway. *Cold Spring Harb. Perspect. Biol.* 5:a013334. https://doi.org/10.1101/cshperspect.a013334

Favaloro, V., M. Spasic, B. Schwappach, and B. Dobberstein. 2008. Distinct targeting pathways for the membrane insertion of tail-anchored (TA) proteins. *J. Cell Sci.* 121:1832–1840. https://doi.org/10.1242/jcs.020321

Fredrickson, E.K., P.S. Gallagher, S.V. Clowes Candadai, and R.G. Gardner. 2013. Substrate recognition in nuclear protein quality control degradation is governed by exposed hydrophobicity that correlates with aggregation and insolubility. *J. Biol. Chem.* 288:6130–6139. https://doi.org/10.1074/jbc.M112.406710

Guna, A., N. Volkmar, J.C. Christianson, and R.S. Hegde. 2018. The ER membrane protein complex is a transmembrane domain insertase. *Science.* 359:470–473. https://doi.org/10.1126/science.aao3099

Hassink, G.C., B. Zhao, R. Sompallae, M. Altun, S. Gastaldello, N.V. Zinin, M.G. Masucci, and K. Lindsten. 2009. The ER-resident ubiquitin-specific protease 19 participates in the UPR and rescues ERAD substrates. *EMBO Rep.* 10:755–761. https://doi.org/10.1038/embor.2009.69

Hegde, R.S., and R.J. Keenan. 2011. Tail-anchored membrane protein insertion into the endoplasmic reticulum. *Nat. Rev. Mol. Cell Biol.* 12:787–798. https://doi.org/10.1038/nrm3226

Hegde, R.S., and E. Zavodszky. 2019. Recognition and Degradation of Mislocalized Proteins in Health and Disease. *Cold Spring Harb. Perspect. Biol.* 11:a033902. https://doi.org/10.1101/cshperspect.a033902

Hessa, T., A. Sharma, M. Mariappan, H.D. Eshleman, E. Gutierrez, and R.S. Hegde. 2011. Protein targeting and degradation are coupled for elimination of mislocalized proteins. *Nature.* 475:394–397. https://doi.org/10.1038/nature10181

Kanda, S., K. Yanagitani, Y. Yokota, Y. Esaki, and K. Kohno. 2016. Autonomous translational pausing is required for XBP1u mRNA recruitment to the ER via the SRP pathway. *Proc. Natl. Acad. Sci. USA.* 113:E5886–E5895. https://doi.org/10.1073/pnas.1604435113

Komander, D., and M. Rape. 2012. The ubiquitin code. *Annu. Rev. Biochem.* 81:203–229. https://doi.org/10.1146/annurev-biochem-060310-170328

Kutay, U., E. Hartmann, and T.A. Rapoport. 1993. A class of membrane proteins with a C-terminal anchor. *Trends Cell Biol.* 3:72–75. https://doi.org/10.1016/0962-8924(93)90066-A

Kutay, U., G. Ahnert-Hilger, E. Hartmann, B. Wiedenmann, and T.A. Rapoport. 1995. Transport route for synaptobrevin via a novel pathway of insertion into the endoplasmic reticulum membrane. *EMBO J.* 14:217–223. https://doi.org/10.1002/j.1460-2075.1995.tb06994.x

Lee, J.G., W. Kim, S. Gygi, and Y. Ye. 2014. Characterization of the deubiquitinating activity of USP19 and its role in endoplasmic reticulum-associated degradation. *J. Biol. Chem.* 289:3510–3517. https://doi.org/10.1074/jbc.M113.538934

Leznicki, P., A. Clancy, B. Schwappach, and S. High. 2010. Bat3 promotes the membrane integration of tail-anchored proteins. *J. Cell Sci.* 123: 2170–2178. https://doi.org/10.1242/jcs.066738

Lu, X.Y., X.J. Shi, A. Hu, J.Q. Wang, Y. Ding, W. Jiang, M. Sun, X. Zhao, J. Luo, W. Qi, and B.L. Song. 2020. Feeding induces cholesterol biosynthesis via the mTORC1-USP20-HMGCR axis. *Nature.* 588:479–484. https://doi.org/10.1038/s41586-020-2928-y

Mali, P., K.M. Esvelt, and G.M. Church. 2013. Cas9 as a versatile tool for engineering biology. *Nat. Methods.* 10:957–963. https://doi.org/10.1038/nmeth.2649

Mariappan, M., X. Li, S. Stefanovic, A. Sharma, A. Mateja, R.J. Keenan, and R.S. Hegde. 2010. A ribosome-associating factor chaperones tail-anchored membrane proteins. *Nature.* 466:1120–1124. https://doi.org/10.1038/nature09296

Minami, R., A. Hayakawa, H. Kagawa, Y. Yanagi, H. Yokosawa, and H. Kawahara. 2010. BAG-6 is essential for selective elimination of defective proteasomal substrates. *J. Cell Biol.* 190:637–650. https://doi.org/10.1083/jcb.200908092

Mock, J.Y., J.W. Chartron, M. Zaslaver, Y. Xu, Y. Ye, and W.M. Clemons Jr. 2015. Bag6 complex contains a minimal tail-anchor-targeting module and a mock BAG domain. *Proc. Natl. Acad. Sci. USA.* 112:106–111. https://doi.org/10.1073/pnas.1402745112

Murphy, S.E., and T.P. Levine. 2016. VAP, a Versatile Access Point for the Endoplasmic Reticulum: Review and analysis of FFAT-like motifs in the VAPome. *Biochim. Biophys. Acta.* 1861(8, 8 Pt B):952–961. https://doi.org/10.1016/j.bbalip.2016.02.009

Ordureau, A., J.A. Paulo, J. Zhang, H. An, K.N. Swatek, J.R. Cannon, Q. Wan, D. Komander, and J.W. Harper. 2020. Global Landscape and Dynamics of Parkin and USP30-Dependent Ubiquitylomes in iNeurons during Mitophagic Signaling. *Mol. Cell.* 77:1124–1142.e10. https://doi.org/10.1016/j.molcel.2019.11.013

Phu, L., C.M. Rose, J.S. Tea, C.E. Wall, E. Verschueren, T.K. Cheung, D.S. Kirkpatrick, and B. Bingol. 2020. Dynamic Regulation of Mitochondrial Import by the Ubiquitin System. *Mol. Cell.* 77:1107–1123.e10. https://doi.org/10.1016/j.molcel.2020.02.012

Plumb, R., Z.R. Zhang, S. Appathurai, and M. Mariappan. 2015. A functional link between the co-translational protein translocation pathway and the UPR. *eLife.* 4:e07426. https://doi.org/10.7554/eLife.07426

Rabu, C., P. Wipf, J.L. Brodsky, and S. High. 2008. A precursor-specific role for Hsp40/Hsc70 during tail-anchored protein integration at the endoplasmic reticulum. *J. Biol. Chem.* 283:27504–27513. https://doi.org/10.1074/jbc.M804591200

Ran, F.A., P.D. Hsu, J. Wright, V. Agarwala, D.A. Scott, and F. Zhang. 2013. Genome engineering using the CRISPR-Cas9 system. *Nat. Protoc.* 8: 2281–2308. https://doi.org/10.1038/nprot.2013.143

Rapoport, T.A. 2007. Protein translocation across the eukaryotic endoplasmic reticulum and bacterial plasma membranes. *Nature.* 450:663–669. https://doi.org/10.1038/nature06384

Rodrigo-Brenni, M.C., E. Gutierrez, and R.S. Hegde. 2014. Cytosolic quality control of mislocalized proteins requires RNF126 recruitment to Bag6. *Mol. Cell.* 55:227–237. https://doi.org/10.1016/j.molcel.2014.05.025

Shamas-Din, A., J. Kale, B. Leber, and D.W. Andrews. 2013. Mechanisms of action of Bcl-2 family proteins. *Cold Spring Harb. Perspect. Biol.* 5: a008714. https://doi.org/10.1101/cshperspect.a008714

Shao, S., and R.S. Hegde. 2011. Membrane protein insertion at the endoplasmic reticulum. *Annu. Rev. Cell Dev. Biol.* 27:25–56. https://doi.org/10.1146/annurev-cellbio-092910-154125

Shao, S., and R.S. Hegde. 2016. Target Selection during Protein Quality Control. *Trends Biochem. Sci.* 41(2):124–137. . https://doi.org/10.1016/j.tibs.2015.10.007

Shao, S., M.C. Rodrigo-Brenni, M.H. Kivlen, and R.S. Hegde. 2017. Mechanistic basis for a molecular triage reaction. *Science.* 355:298–302. https://doi.org/10.1126/science.aah6130

Sharma, A., M. Mariappan, S. Appathurai, and R.S. Hegde. 2010. In vitro dissection of protein translocation into the mammalian endoplasmic reticulum. *Methods Mol. Biol.* 619:339–363. https://doi.org/10.1007/978-1-60327-412-8_20

Stefanovic, S., and R.S. Hegde. 2007. Identification of a targeting factor for posttranslational membrane protein insertion into the ER. *Cell.* 128: 1147–1159. https://doi.org/10.1016/j.cell.2007.01.036

Südhof, T.C., and J.E. Rothman. 2009. Membrane fusion: grappling with SNARE and SM proteins. *Science.* 323:474–477. https://doi.org/10.1126/science.1161748

Sundaram, A., R. Plumb, S. Appathurai, and M. Mariappan. 2017. The Sec61 translocon limits IRE1α signaling during the unfolded protein response. *eLife.* 6:e27187. https://doi.org/10.7554/eLife.27187

Thorne, C., R.L. Eccles, J.M. Coulson, S. Urbé, and M.J. Clague. 2011. Isoform-specific localization of the deubiquitinase USP33 to the Golgi apparatus. *Traffic.* 12:1563–1574. https://doi.org/10.1111/j.1600-0854.2011.01261.x

Vilardi, F., H. Lorenz, and B. Dobberstein. 2011. WRB is the receptor for TRC40/Asna1-mediated insertion of tail-anchored proteins into the ER membrane. *J. Cell Sci.* 124:1301–1307. https://doi.org/10.1242/jcs.084277

Wang, F., E.C. Brown, G. Mak, J. Zhuang, and V. Denic. 2010. A chaperone cascade sorts proteins for posttranslational membrane insertion into the endoplasmic reticulum. *Mol. Cell.* 40:159–171. https://doi.org/10.1016/j.molcel.2010.08.038

Xu, Y., D.E. Anderson, and Y. Ye. 2016. The HECT domain ubiquitin ligase HUWE1 targets unassembled soluble proteins for degradation. *Cell Discov.* 2:16040. https://doi.org/10.1038/celldisc.2016.40

Yamamoto, Y., and T. Sakisaka. 2012. Molecular machinery for insertion of tail-anchored membrane proteins into the endoplasmic reticulum membrane in mammalian cells. *Mol. Cell.* 48:387–397. https://doi.org/10.1016/j.molcel.2012.08.028

Yanagitani, K., Y. Kimata, H. Kadokura, and K. Kohno. 2011. Translational pausing ensures membrane targeting and cytoplasmic splicing of XBP1u mRNA. *Science.* 331:586–589. https://doi.org/10.1126/science.1197142

Yau, R.G., K. Doerner, E.R. Castellanos, D.L. Haakonsen, A. Werner, N. Wang, X.W. Yang, N. Martinez-Martin, M.L. Matsumoto, V.M. Dixit, and M. Rape. 2017. Assembly and Function of Heterotypic Ubiquitin Chains in Cell-Cycle and Protein Quality Control. *Cell.* 171:918–933.e20. https://doi.org/10.1016/j.cell.2017.09.040

Zhang, X., and S.O. Shan. 2014. Fidelity of cotranslational protein targeting by the signal recognition particle. *Annu. Rev. Biophys.* 43:381–408. . https://doi.org/10.1146/annurev-biophys-051013-022653

Zhang, Z.R., J.S. Bonifacino, and R.S. Hegde. 2013. Deubiquitinases sharpen substrate discrimination during membrane protein degradation from the ER. *Cell.* 154(3):609–622. . https://doi.org/10.1016/j.cell.2013.06.038

JCB

Supplemental material

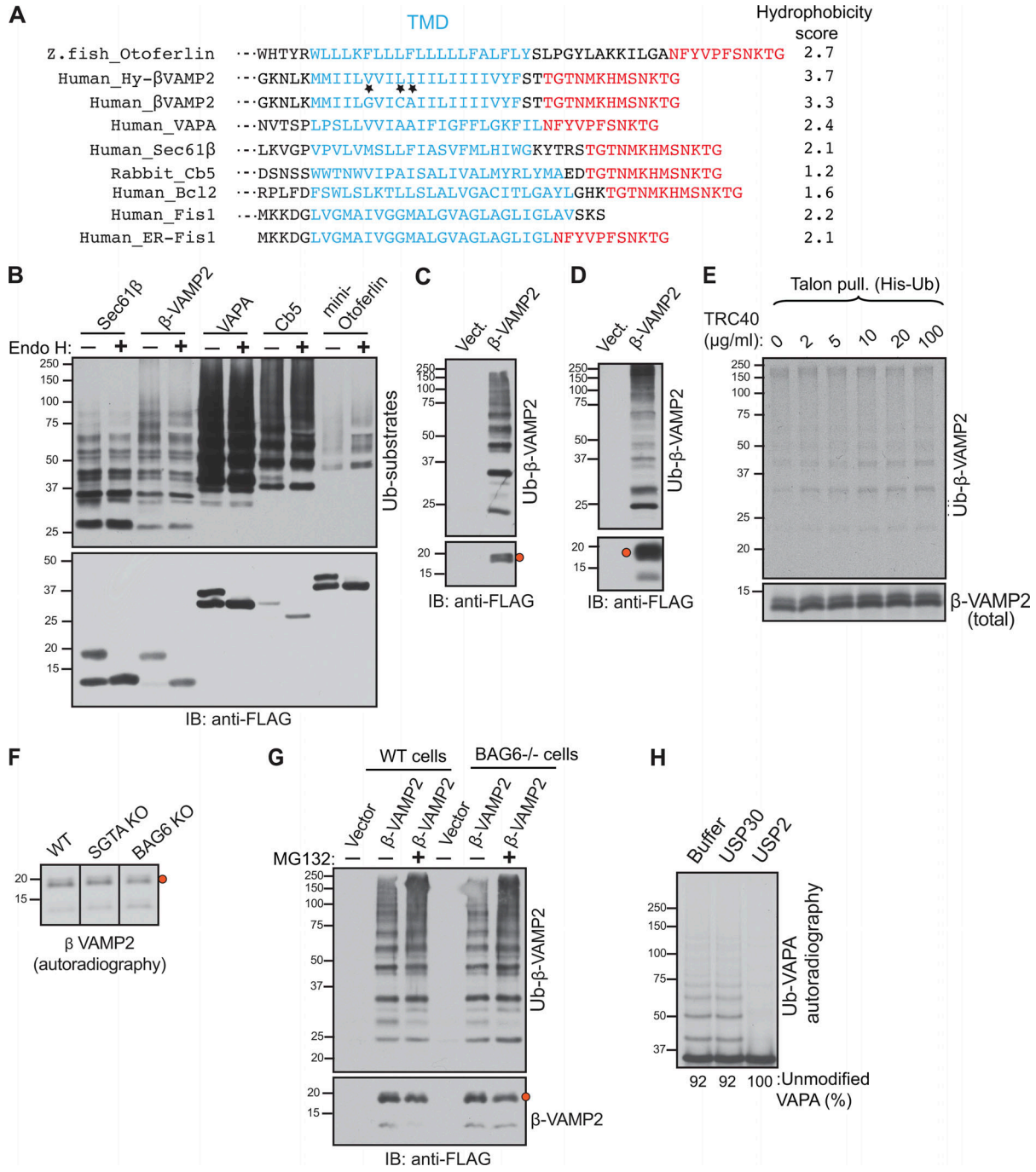

Figure S1. **Characterization of TA protein ubiquitination in the cytosol. (A)** The TMD sequences of the indicated proteins are shown in blue. The red text denotes the glycosylation tag. The TMD hydrophobicity score was calculated using the grand average hydropathy calculator. Hydrophobic (Hy)-β-VAMP2 was created by replacing less hydrophobic residues with hydrophobic amino acids in the TMD of VAMP2. The star indicates mutations in β-VAMP2-Hy. ER-Fis1 was created by replacing the last three amino acids of Fis1 with an N-glycosylation site. **(B)** The indicated constructs were immunoprecipitated with anti-FLAG beads and boiled in 1% SDS buffer. Samples were diluted and incubated without or with Endo H. The samples were immunoblotted (IB) for ubiquitin (Ub) substrates via anti-HA antibody and TA substrates via anti-FLAG antibody. **(C)** Lysis buffer containing 1% SDS was heated to 95°C and added directly to the plated cells expressing β-VAMP2 and HA-ubiquitin. The buffer was diluted down to 0.1% SDS, and β-VAMP2 was immunoprecipitated and analyzed as in B. **(D)** HEK293 cells stably expressing β-VAMP2 were transiently transfected with HA-ubiquitin and lysed with RIPA. β-VAMP2 was immunoprecipitated and analyzed as in B. **(E)** β-VAMP2–encoding transcripts were in vitro translated in RRL, including increasing concentrations of purified TRC40. The samples were either immunoprecipitated for β-VAMP2 with anti-FLAG antibodies or isolated for ubiquitin-conjugated TA proteins using Talon resin and analyzed by SDS-PAGE autoradiography. **(F)** WT, SGTA$^{-/-}$, or BAG6$^{-/-}$ cells were transfected with β-VAMP2 and radiolabeled for 30 min and chased for 2 h. β-VAMP2 was immunoprecipitated and analyzed via SDS-PAGE autoradiography. **(G)** WT or BAG6$^{-/-}$ cells were transfected with β-VAMP2. The cells were then treated with either 20 μM MG132 or no treatment for 4 h and were analyzed as in C. **(H)** Radiolabeled VAPA was immunoprecipitated via its FLAG tag and treated with buffer, purified recombinant USP30, or USP2, and analyzed by autoradiography. The unmodified VAPA was quantified and USP2-treated VAPA was set as 100%.

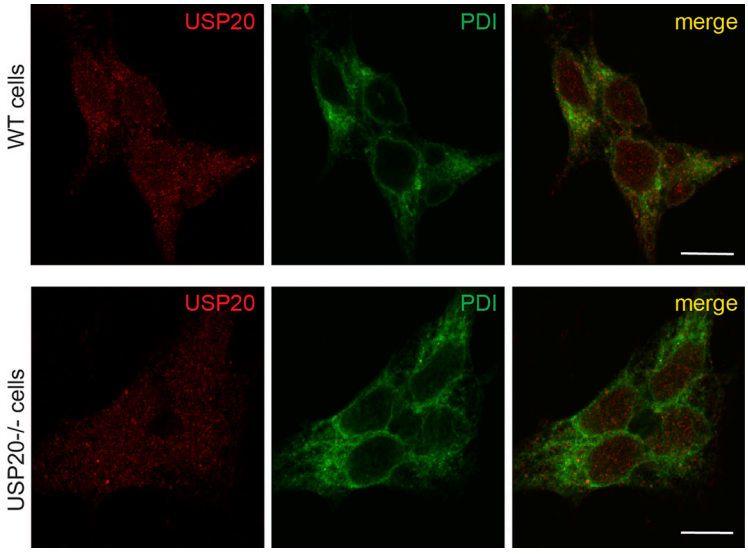

Figure S2. **Endogenous USP20 localization.** Either WT or USP20$^{-/-}$ HEK293 cells were fixed with 3.7% formaldehyde and permeabilized in 0.1% Triton X-100. The cells were stained with rabbit α-USP20 and mouse α-PDI followed by goat α-rabbit IgG-Cy2 and goat α-mouse IgG-Cy3. The stained cells were examined for colocalization (yellow) of USP20 (red) and PDI (green) by confocal microscopy. Scale bar, 10 µm.

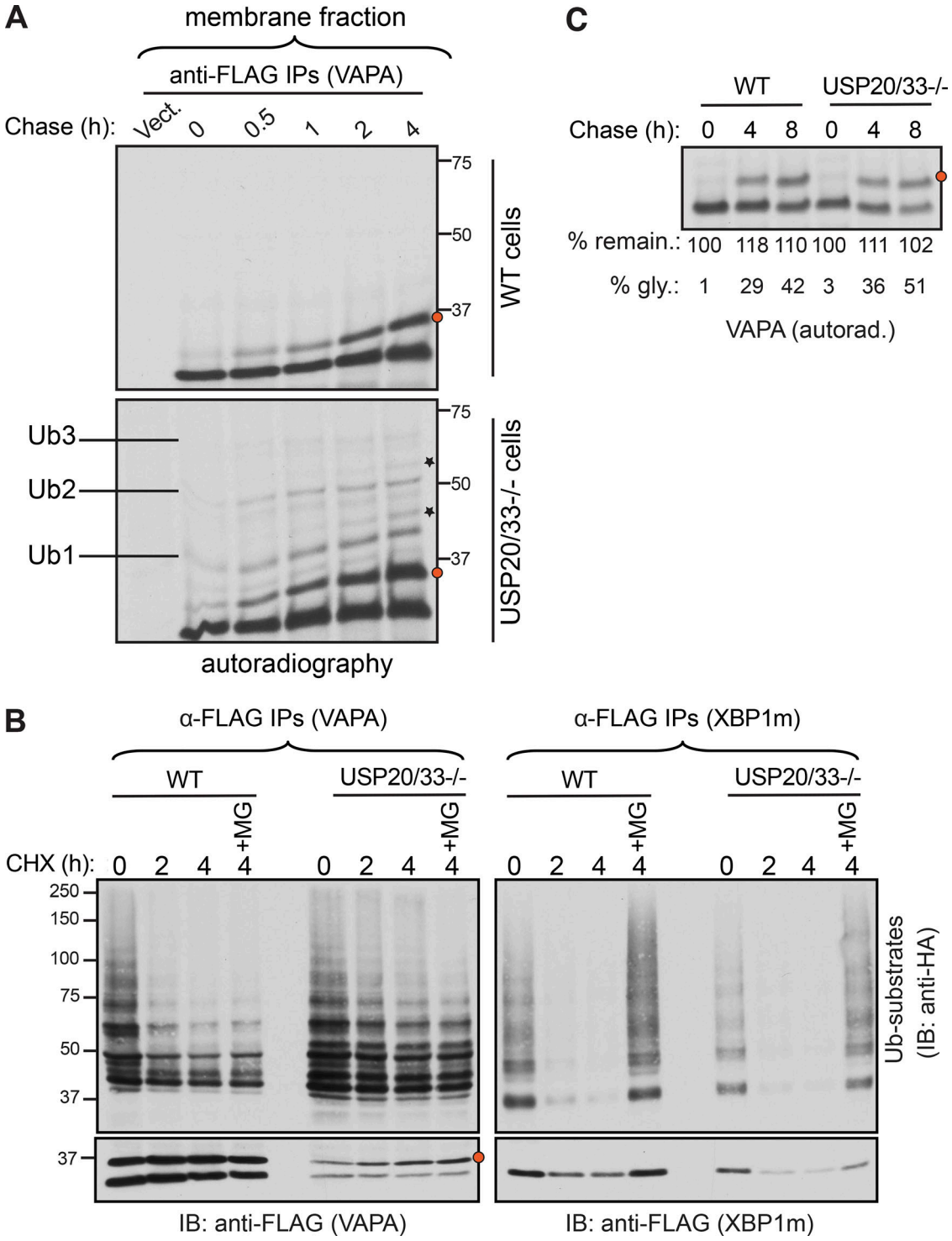

Figure S3. **Ubiquitinated TA proteins accumulate in cells lacking USP20/33. (A)** Cells were transfected with VAPA-FLAG and Ubiquitin-HA and then radiolabeled. Cells were then fractionated into cytosol and membrane with 0.015% digitonin. VAPA was then immunoprecipitated (IP) from the membrane fraction of WT and USP20/33$^{-/-}$ cells and analyzed by autoradiography. The orange circle represents glycosylated VAPA, and the star represents ubiquitinated (Ub) and glycosylated VAPA. **(B)** WT or USP20/33$^{-/-}$ cells expressing VAPA or XBP1m were treated with CHX alone or with proteasome inhibitor MG132 for the indicated durations. VAPA and XBP1m were immunoprecipitated via anti-FLAG antibody beads and analyzed by immunoblotting (IB) with anti-FLAG for substrates and anti-HA antibody for ubiquitinated substrates. **(C)** FLAG-tagged VAPA-expressing cells were metabolically labeled and chased for the indicated time points. Cell lysates were immunoprecipitated with anti-FLAG beads and analyzed by SDS-PAGE autoradiography (autorad.). The protein level at 0 h time point was taken as 100%, and the percentage of the remaining protein was calculated with respect to 0 h. The percentage of the glycosylated (gly) band from total was quantified using ImageJ and shown under the blot.